

Contents lists available at ScienceDirect

Applied Energy

journal homepage: www.elsevier.com/locate/apen



Flying electric: A comparative analysis of spare part demands and material cost for all-electric, hybrid-electric, and conventional aircraft propulsion systems

Jan-Alexander Wolf* O, Robert Meissner O, Ahmad Ali Pohya O, Gerko Wende O

Institute of Maintenance, Repair and Overhaul, German Aerospace Center, Hein-Saß-Weg 22, 21129 Hamburg, Germany

HIGHLIGHTS

- · A novel methodology for estimating material cost of electric aircraft is introduced.
- · A degradation model is used to estimate maintenance intervals of battery cells.
- · Battery sizing and temperature management are levers for optimizing maintenance costs.
- · Hybrid-electric concepts are expected to be more economically viable than all-electric concepts.

ARTICLE INFO

Keywords: Electric aircraft Hybrid electric Aircraft maintenance Lithium-ion battery Battery degradation Reliability Cost analysis

ABSTRACT

The aviation industry is driven by its pursuit of a cleaner and more sustainable ecosystem while continually growing in passenger volume and emissions on a global level. While current aero-engines have already reached their limits in terms of efficiency optimization, revolutionary drivetrain technologies such as battery-powered propulsion systems promise to significantly reduce emissions. However, besides the technological challenges such as low gravimetric energy densities for battery storage systems, a potential adoption of these technologies is further hampered by uncertainties about operational availability and maintenance costs. Therefore, with this work, we address parts of that knowledge gap by quantifying the expected changes in material costs and part replacements for the maintenance of battery-powered All-Electric Aircraft (AEA) and Hybrid-Electric Aircraft (HEA) propulsion systems. For this purpose, we establish a cost estimation method, which is based on expected reliability metrics for the corresponding drivetrain components and resulting spare part demand. Special focus is given to design and operating recommendations for the battery storage unit through the application of a degradation model. As a consequence, we can identify appropriate over-sizing ratios and operating temperatures to optimize the resulting maintenance costs of the battery system. By carrying out a comparative analysis with a conventional propulsion system, we can observe an expected increase in maintenance-related material costs of 163 % for AEA and 26 % for HEA configurations, respectively. Therefore, with the results from this study being fed-back to early design iterations, we can support the development of technically-feasible and economicallysustainable electric aircraft design concepts.

1. Introduction

In its pursuit of a cleaner and more sustainable ecosystem, the aviation industry has undergone a fundamental transformation in recent years that will continue to shape the future development of the sector. Following a temporary drop during the global coronavirus pandemic, air transport is now once again characterized by strong growth in passenger

volumes and high absolute emissions [1]. Although aviation currently accounts for a minor part of the world's annual CO_2 emissions [2,3], this share is likely to increase in the coming years as other industries are continuously reducing their impact. In addition, an aircraft generates significant non- CO_2 emissions (such as nitrogen oxides, soot, water vapor, and sulfate aerosols) that have climate damaging effects as well as

^{*} Corresponding author.

Email address: jan-alexander.wolf@dlr.de (J.-A. Wolf).

Nomen	clature	FQIC	Fuel Quantity Indication Computer	
		GCU	Generator Control Unit	
Acronyms		HDS	Hybrid Distribution System	
AC	Alternating Current	HEA	Hybrid-Electric Aircraft	
AEA	All-Electric Aircraft	HPS	Hybrid Propulsion System	
APU	Auxiliary Power Unit	HSS	Hybrid Storage System	
ATA	Air Transport Association	HTS	High-Temperature Superconductivity	
ATR	Avions de Transport Régional	IDG	Integrated Drive Generator	
BCS	Battery Cooling System	LIB	Lithium-Ion Battery	
BMS	Battery Management System	LLP	Life Limited Part	
CDS	Conventional Distribution System	LRU	Line-Replaceable Unit	
CPS	Conventional Propulsion System	MCS	Motor Cooling System	
CSS	Conventional Storage System	MPD	Maintenance Planning Document	
DC	Direct Current	MRO	Maintenance, Repair and Overhaul	
DLR	Deutsches Zentrum für Luft- und Raumfahrt	MTBF	Mean Time Between Failure	
DMC	Direct Maintenance Cost	MTBUR	Mean Time Between Unscheduled Removal	
DOC	Direct Operating Cost	MTOW	Maximum Takeoff Weight	
DOD	Depth Of Discharge	NFF	No Fault Found	
ECU	Electronic Control Unit	PMSM	Permanent-Magnet Synchronous Motor	
EDS	Electric Distribution System	QPA	Quantity Per Aircraft	
EOL	End of Life	RCM	Reliability Centered Maintenance	
EPS	Electric Propulsion System	SAF	Sustainable Aviation Fuel	
ESS	Electric Storage System	SOC	State Of Charge	
FC	Flight Cycle	SRU	Shop-Replaceable Unit	
FH	Flight Hour	SVC	Shop Visit Cost	
FOD	Foreign Object Damage	TRU	Thrust Reverser Unit	

other harmful effects on the environment [1,4]. This impact is reflected by ambitious climate goals and the need for concrete countermeasures, e.g., the Green Deal initiative of the European Commission [5]. With one of its key objectives being climate neutrality by 2050, it becomes apparent that substantial operational optimizations and technological developments will be required for a sustainable future air transport system.

Consequently, a great effort has been made in recent decades to improve fuel efficiency, e.g., by improvements in aircraft aerodynamics, structural weight, and engine performance [6,7]. Whereas an increase in efficiency of the engine was the most promising approach for a long time, the maturity of contemporary technologies has almost reached its limits today and only minor improvements can be expected for conventional engines in the future [8]. Therefore, as the goal of climate neutrality appears to be incompatible with conventional aircraft designs, alternative propulsion concepts have received significant attention in aviation research recently. The most common approaches here are the use of Sustainable Aviation Fuel (SAF) [9] or liquid hydrogen [10] as alternative fuels as well as the electrification of drive systems through hydrogen-powered fuel cells [11] or battery storage [12], respectively. While battery-electric systems in particular face substantial technological challenges, e.g., excessive system masses due to low gravimetric energy densities [13-15], they offer higher efficiencies and specific power compared to fuel cell systems [16]. For example, current batteries can achieve efficiencies of 80 % to 95 %, whereas fuel cells typically transform 40 % to 60 % of the hydrogen-stored energy into electrical power [17-19].

Since the availability of renewable energy for air transport is limited and needs to be used as efficiently as possible [20], we will focus our work on battery-electric concepts, i.e., All-Electric Aircraft (AEA) and Hybrid-Electric Aircraft (HEA) configurations.

In case of an AEA, the entire energy demand of the propulsion system is provided by electric motors, eliminating the kerosene combustion with the corresponding avoidance of direct emissions during the flight. However, due to the low energy density of current battery technologies,

this concept is mainly feasible for smaller aircraft. Consequently, for larger aircraft with high energy demands, the HEA concept is a suitable alternative, where electric motors are combined with conventional engines to generate propulsion. The configurations allow electric motors to provide additional power during flight segments with high thrust demands, e.g., during take-off, while the conventional combustion engine can be downsized and optimized for cruise segments [21].

Besides existing technological challenges, the required rapid market ramp-up of these new drive systems is also hampered by economic uncertainties. Especially for a cost-driven industry such as aviation with its long development phases and high safety standards, the introduction of revolutionary technological innovations is associated with high economic risks [22]. Therefore, to mitigate reluctance of manufacturers and operators, a cost estimation in early design stages is essential. While cost uncertainties can be attributed to a number of factors, one of the more relevant aspects is maintenance – as Direct Maintenance Cost (DMC) accounts for up to 20 % of an airline's Direct Operating Cost (DOC) [14]. Taking a closer look at the DMC shows labor and material costs as main contributors, with the latter accounting for roughly 46 % of a Maintenance, Repair and Overhaul (MRO) provider's cost [23].

Aircraft maintenance also has a strong secondary impact on operating costs, as it influences aircraft availability and operational reliability of a fleet. Over a 12-year period, a short- to medium-haul aircraft can be expected to spend between 40 and 68 days on the ground for scheduled maintenance alone [24]. Additionally, uncertainties in maintenance tasks and the unavailability of spare parts can lead to significant unexpected disruptions in flight operations [25]. Maintenance can account for up to 13 % of all flight delays, with long-lasting delays being particularly affected [26]. This could be even more severe in the case of battery-powered aircraft, as batteries require regular replacements and maintenance requirements are unknown due to a lack of operational experience. It is therefore important to take these changes into account in fleet planning and spare part inventory management. In an initial phase, the repair and replacement frequencies due to component failures or degradation can serve as useful indicators in this regard.

While there are DOC-based methods to conduct economic comparisons between different aircraft concepts [27,28], they are typically based on regression analyses of airline fleet and financial data. These methods primarily consider data of conventional aircraft configurations, which limits their applicability to new or unconventional system designs [29]. Therefore, there are only a few studies on DOC assessments of electric aircraft concepts that aim to provide a more comprehensive estimate of the maintenance costs. For example, Finger et al. [30] provided an overview of cost estimation methods for hybrid-electric aircraft, but maintenance costs were not adjusted in comparison to aircraft with conventional propulsion systems. Monjon and Freire [31] derived the operating costs for an regional AEA; however, the method is based on 1990s turbine-powered transport aircraft and no correction factors were applied to the maintenance costs. Although costs due to battery replacement were taken into account, only a standard replacement interval of 2000 Flight Cycles (FCs) was assumed, without considering missionspecific degradation effects. Schäfer et al. [32] estimated the changes in maintenance costs of an all-electric A320-equivalent mainly based on the replacement costs of the battery, assuming a standard replacement interval of 5000 FCs without an extensive analysis of the useful battery life. Scholz et al. [33] conducted an operating cost analysis of an AEA after modifying the maintenance cost calculation of the electric powertrain. However, the electric system was not analyzed in detail and it was assumed that the costs correspond to a fixed proportion of 75 % of the conventional reference system.

Additionally, many scientific studies tend to focus on safety and certification issues [34–36] and neglect maintenance implications for different design solutions of battery systems. Consequently, despite the perception of batteries being a substantial driver for the maintenance efforts [1,31–33,37], there is currently no reliable information available on how electrified drive systems in aviation will affect the maintenance-related material costs. Lastly, several studies have investigated the expected changes in maintenance of conventional turbofan engines in HEA configurations [38–40], but they lack a holistic cost estimation for the entire drive system with all its accessories.

Considering these limitations, we want to address the following key aspects in our work.

- Establishment of a novel reliability-based methodology to assess the expected changes in maintenance-related material costs for AEA and HEA to identify their main cost drivers.
- Analysis of different battery operating scenarios to identify essential degradation factors and to derive recommendations for optimized maintenance-related costs.
- Analysis of the maintenance effects for HEA design concepts with special focus on trade-offs between cost savings for the conventional engine and additional material costs for the electric drivetrain.

For our study, an Airbus A320 is used as conventional, kerosene-powered reference system since it is the predominant passenger aircraft alongside Boeing's 737 [41]. With single-aisle models for short-to-medium flight segments being a continuously increasing factor in the world fleet [42], an economically-competitive electrified aircraft design provides substantial environmental leverage. Therefore, the comparative analysis of our work will provide a valuable contribution to the assessment of cost efficiencies for alternative propulsion systems. Furthermore, the results allow aircraft designers and operators to gain insights into the maintenance characteristics of battery systems in aviation, building the foundation for a potential technology integration.

The remainder of this paper is structured as follows. After presenting the theoretical fundamentals of a reliability-based maintenance assessment in Section 2, we will introduce the drive configurations and their components in Section 3. This is followed by a characterization of the battery systems in Section 4, whose influence is given a special focus in our work. On this basis, we will develop a method for analyzing the maintenance scope of different drive systems with regard to the spare part demand in Section 5. By applying this methodology, we will provide

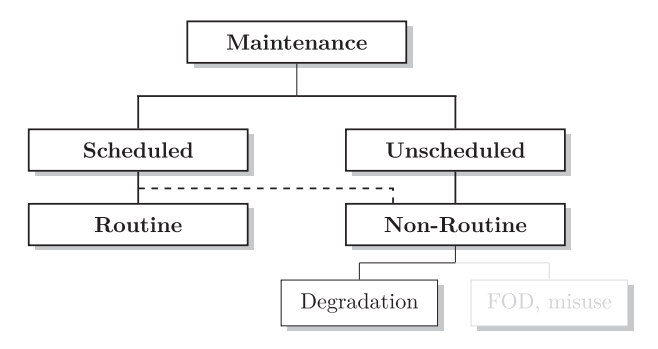


Fig. 1. Schematic representation of the subdivision of maintenance tasks.

a detailed overview of the material costs for the individual components in Section 6. Finally, we will compare the cost efficiency of the drive systems and derive design and operating recommendations from this in Section 7.

2. Fundamentals to estimate material costs in maintenance

Aircraft maintenance is based on the concept of Reliability Centered Maintenance (RCM) [43], where maintenance tasks are defined by the impact of corresponding system failures on functionality and safety. Following this approach, our methodology for assessing the changes in maintenance-related material costs is based on the reliability of the drivetrain components. For this section, we will first specify the scope of our analysis by introducing different categories of maintenance tasks. We will then establish the basis of our methodology by presenting important metrics for the reliability assessment of components.

2.1. Categorization of maintenance tasks

Maintenance is the combination of all technical, administrative, and managerial actions that ensure the functional condition of an item [44]. In a first instance, maintenance measures can be divided into scheduled and unscheduled tasks, depending on their planning capability (see Fig. 1). Here, scheduled maintenance includes all measures that are carried out according to a defined time schedule or number of utilization units [45], whereas unscheduled maintenance is not carried out based on a fixed schedule. A further subdivision can be made into routine and non-routine maintenance. Routine maintenance includes regular and repeated measures that are defined for each aircraft type in a maintenance program, e.g., a Maintenance Planning Document (MPD) [24]. These tasks can be functional checks or so called discard tasks (e.g., the scheduled replacement of filter elements). In contrast, non-routine maintenance covers all measures that are typically carried out in the event of unexpected failures or malfunctions beyond a prescribed program.

While the majority of scheduled maintenance tasks are visual inspections [46], we focus in this study on overhaul and restoration tasks since these categories are the main drivers of material cost in maintenance [47]. Overhaul tasks include preventive measures to delay signs of degradation and wear, whereas restoration is characterized by corrective tasks in order to restore the functionality of faulty or defective units [44]. In our analysis, the scope of routine tasks is mainly driven by Life Limited Parts (LLPs), i.e., parts that are replaced after a defined service life. On the other hand, typical non-routine tasks considered in our work are failure-related repair or replacement tasks, which are caused by various incidents. First, such a failure may be based on unavoidable physical degradation mechanisms during regular operation and their probability of occurrence increases with the number of operating cycles and the associated applied stresses [45]. Second, a component may fail due to operational misuse or the occurrence of Foreign Object Damage (FOD), e.g., bird strikes or other object impacts. However, since the failure causes are random by nature [48], these events cannot be reliably projected and are excluded from our maintenance analysis. Lastly, it

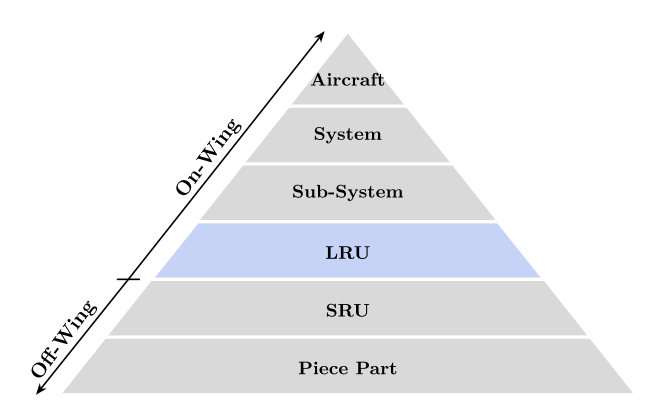


Fig. 2. Schematic representation of the subdivision of aircraft systems into onwing and off-wing.

should be mentioned that non-routine maintenance tasks can also arise out of scheduled maintenance measures [24]. This may be the case if unexpected damage is discovered during a routine task.

Furthermore, our maintenance analysis is carried out at a Line-Replaceable Unit (LRU) level (see Fig. 2), i.e., the smallest coherent unit that can be removed and installed on-wing for repairs or replacement [49]. Therefore, the subsequent off-wing disassembly of these components into Shop-Replaceable Units (SRUs) or piece parts in designated repair centers is outside the scope of this paper. Additionally, there is a lack of (a) information on maintenance of electric drivetrains in aviation, (b) associated labor costs for maintenance task execution, (c) usage rates of consumables (e.g., lubricants), and (d) tool costs, which is why our analysis focuses exclusively on the material cost of the individual components.

2.2. Metrics for the reliability assessment of components

Reliability is the ability of a unit to perform a required function under given conditions for a given time interval [45]; thus, it is one of the most important properties of a unit. If reliability is no longer guaranteed, e.g., due to a failure, the component must be repaired or replaced. The frequency of failure events can be expressed by statistical parameters, with the failure rate in particular being widely used in the aviation industry as a measure of the reliability of a component or system [50]. The failure rate indicates the average number of failures to be expected over a certain time period. It can be derived by the following three methods.

Empirical approach. Statistical values from the real operation are used as the failure rate is determined by relating the measured number of failures of a component to its operating time. To derive the failure rate for components that have not yet been in operation for a longer time period, empirical values from comparable components under similar operating conditions can be used.

Experimental approach. For components without empirical values from real operation, lifetime or accelerated aging tests in a controlled laboratory environment can be conducted. By simulating operating conditions and load cycles, the subsequent failure or degradation behavior can be used as a basis for determining failure rates.

Analytical approach. For novel or unconventional components, analytical models based on empirical or physical evidence can be used to simulate and predict the degradation and failure behavior.

It has to be noted that some components do not have a linear but a more complex failure behavior, which is driven by a combination of different degradation mechanisms. For example, failure rates for power electronics are typically described using so called bathtub curves consisting of three phases (see Fig. 3). While the first phase is characterized

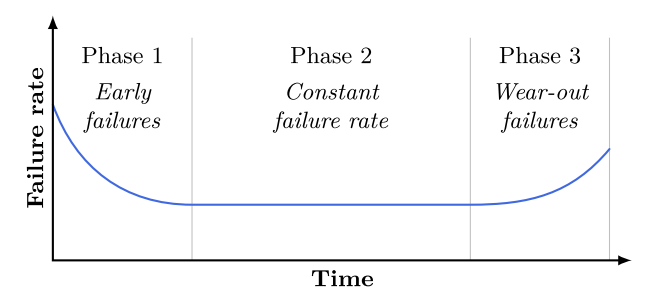


Fig. 3. Bathtub curve, which schematically represents the typical shape of the failure rate as a function of time.

by early failures, the second phase is represented by a low and approximately constant failure rate, ultimately culminating in the third phase with an increased failure rate due to excessive degradation [40,49]. Although the operational utilization of these components is often located in phase 2, in reality the failure rate is not necessarily constant over time [51]. In our study, the component reliability is analyzed on a world-wide fleet level, which consists of both new aircraft at the beginning of their service life and aircraft with many Flight Hours (FHs) performed. For the reference aircraft A320, the world-wide fleet has logged over 357 million total FHs since entry into service [52], with some aircraft still active after more than 30 years and with over 90,000 FHs performed [53]. Due to this very broad fleet, the effects of newer and older components are expected to balance each other so that the assumption of a constant failure rate over time is valid [51].

The analysis in this paper is mainly based on the following reliability measurements of a component. Their respective relationships with each other are shown in Fig. 4.

Mean Time Between Failure (MTBF). The MTBF relates the flight hours of a unit $t_{\rm FH}$ to the number of failures $n_{\rm F}$ that occurred during this period (see Eq. (1)).

$$t_{\rm MTBF} = \frac{t_{\rm FH}}{n_{\rm F}} \tag{1}$$

If the failure rate λ is assumed to be constant, the MTBF can be calculated as the reciprocal of said failure rate (see Eq. (2)) [51].

$$t_{\text{MTBF}} = \frac{1}{\lambda}$$
 with $\lambda(t) = \text{const.}$ (2)

Mean Time Between Unscheduled Removal (MTBUR). The MTBUR relates the FHs to the number of unscheduled removals that are carried out, e.g., due to failure messages. In contrast to MTBF removals, no distinction is made as to whether a defect is actually present or whether no functional impairment can be determined and the component can continue to be used without repair or replacement [24]. This relationship is expressed by the No Fault Found (NFF) rate, which indicates the percentage of removals without recognizable functional impairment in relation to the total number of unplanned removals. The NFF rate thus relates the MTBUR value and the MTBF (see Eq. (3)) [24].

$$r_{\rm NFF} = 1 - \frac{t_{\rm MTBUR}}{t_{\rm MTBF}} \tag{3}$$

With a given NFF rate, the MTBUR value can be transferred to a MTBF value (see Eq. (4)).

$$t_{\rm MTBF} = \frac{t_{\rm MTBUR}}{1 - r_{\rm NFF}} \tag{4}$$

so that

$$t_{\text{MTBUR}} \le t_{\text{MTBF}}$$
 with $r_{\text{NFF}} \ge 0$ (5)

The NFF rate is affected by various factors and generally varies for different types of components within a typical range from 10 % to 60 %

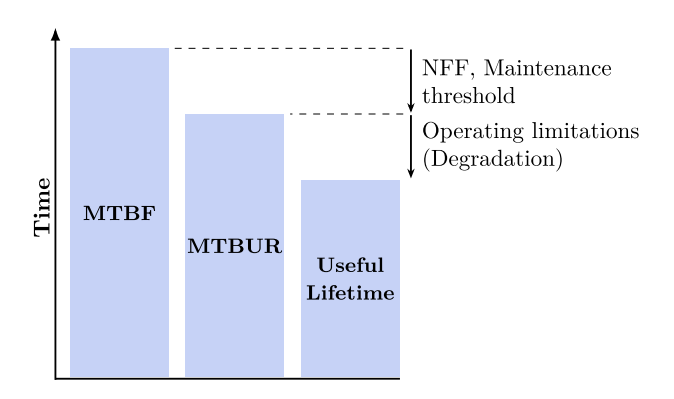


Fig. 4. Temporal relationship between MTBF values, MTBUR values and the useful lifetime.

[24,54,55]. Based on conversations with aircraft manufacturers, we assume a constant NFF rate of 15 % for each component within our study, as this corresponds to the maximum value that is typically specified as a requirement for component suppliers.

Useful lifetime. In addition to failure-based usage limits, other limits must be taken into account for certain components as the End of Life (EOL) can be reached before the component actually fails. This may be the case for components that require a certain level of performance during operation while experiencing performance decreases due to degradation effects, e.g., batteries with decreasing capacities.

Despite the failure rate being widely used for reliability assessments of systems and components, its validity for defining specific maintenance intervals remains controversial [14,51]. Furthermore, the specific reliability value varies significantly depending on the underlying method for its determination since no binding boundary conditions are prescribed for obtaining failure rates. Therefore, it is often not feasible to derive distinct and reliable MTBF values for new components. However, in Section 5.1 we will present an approach for dealing with these strong variations.

3. Introduction to the drive configurations

Electric drive systems and their components differ significantly from conventional systems and introduce multiple uncertainties regarding their technology, reliability, and costs. Since no larger battery-powered aircraft is in commercial operation yet, the following section is dedicated to the brief introduction of the reference aircraft alongside a definition of the electric drive configurations.

3.1. Baseline operating scenarios

As mentioned in Section 1, our analysis of material cost implications for an electric drive system is based on a comparison to a conventional Airbus A320. The A320 family is a series of narrow-body airliners, powered by two conventional turbofan engines. The baseline model has a maximum capacity of up to 180 passengers and a maximum takeoff mass of 78 t [56]. Most of the versions currently in service are equipped with the CFM56-5B4 engine model from the manufacturer CFM International [57]. In this study, the operating scenarios in Table 1 serve as reference values that are comparable to the mission profile of an A320 [41,58]. The characteristic values are given in Flight Cycle (FC) and Flight Hour (FH).

In our work, the electric systems are designed for an application on this reference aircraft. The A320 provides a reliable data basis for our analysis, despite smaller aircraft with lower range and payload generally being considered more suitable for electric propulsion due to their smaller battery size. Considering these circumstances, the basic design of the full-electric and hybrid-electric architecture described below has

Table 1Operating scenarios as references for the investigated aircraft models [59].

Flight scenario	Annual utilization	Average flight time
Short segments World average	2750 FC/a 1500 FC/a	1.0 FH/FC 1.8 FH/FC
Long segments	917 FC/a	3.0 FH/FC

therefore been chosen so that it can be applied to most aircraft types. An application to other aircraft sizes or different ranges would then require an adjustment of the component sizing and spare part price (see Table 4) depending on the maximum power of the aircraft. The battery sizing is particularly relevant here, where the required number of battery cells is determined based on the maximum power and energy requirements of the flight mission (see Section 4.2).

3.2. Electric drive configurations

With the specifications of the conventional system layout discussed, we want to define the electric drive system next. In order to evaluate the drive configuration's reliability, the corresponding components need a certain level of technological maturity to provide the required failure rate data (see Section 2.2). For example, despite its high potential for the implementation of electric propulsion systems [8], we do not consider High-Temperature Superconductivity (HTS) systems due to its limited data availability. We also want to highlight that the underlying AEA and HEA system designs are based on preliminary assumptions. Therefore, a reiteration of compliance with current certification standards for the assumed design solution has been outside the scope of this paper.

In order to determine the number of drive motors, it is taken into account that today's electric motors for aviation are limited to about half the power densities of conventional turbofan engines [60]. Consequently, for an initial AEA concept, we assume a design of four electric motors, each of them providing propulsion through a propeller. Furthermore, each motor needs to be supplied with electric energy by a distribution line corresponding to the layout in Fig. 5. In addition, the components for the energy supply of secondary systems (e.g., avionics, air conditioning, and de-icing) are not further analyzed in this study since they most likely remain unaffected by the changes to the propulsion system.

For the HEA layout, a parallel electric drive to the conventional kerosene-powered engine configuration seems appropriate, with this design requiring comparatively few adjustments to the drive layout. The most common parallel approach consists of integrating an electric motor on the low-pressure shaft of the conventional gas turbine in order to provide additional mechanical power or to drive the shaft fully electrically during individual mission segments [8]. For the HEA in this study, thrust generation is still provided by two conventional turbofan engines with support of an electric motor on each. The electric drivetrain corresponds to the basic layout of the AEA configuration in Fig. 5, except for the installation of propellers. The electric drivetrain can be subdivided into the following systems with respect to their respective functions.

Electric Storage System (ESS). The components of the ESS are responsible for storing chemical energy and converting it into electrical energy. The system consists of a rechargeable battery pack, a Battery Management System (BMS), and a Battery Cooling System (BCS). The BMS controls the storage unit and ensures a balanced operation, so that no battery cell is loaded beyond the specified manufacturer limits during charging and discharging [62]. A BCS is required to regulate operating temperatures of the battery within a permitted range. We define the BCS for this study as a liquid cooling system. Liquid-based systems are characterized by high cooling performance and stable temperature control [63,64]. Furthermore, they are already being used in general aviation, e.g., for the Pipistrel Velis Electro [65]. For simplification, it is assumed that the cooling system consists of the main sub-components pump, heat exchanger, and piping. Due to redundancy and safety requirements, the

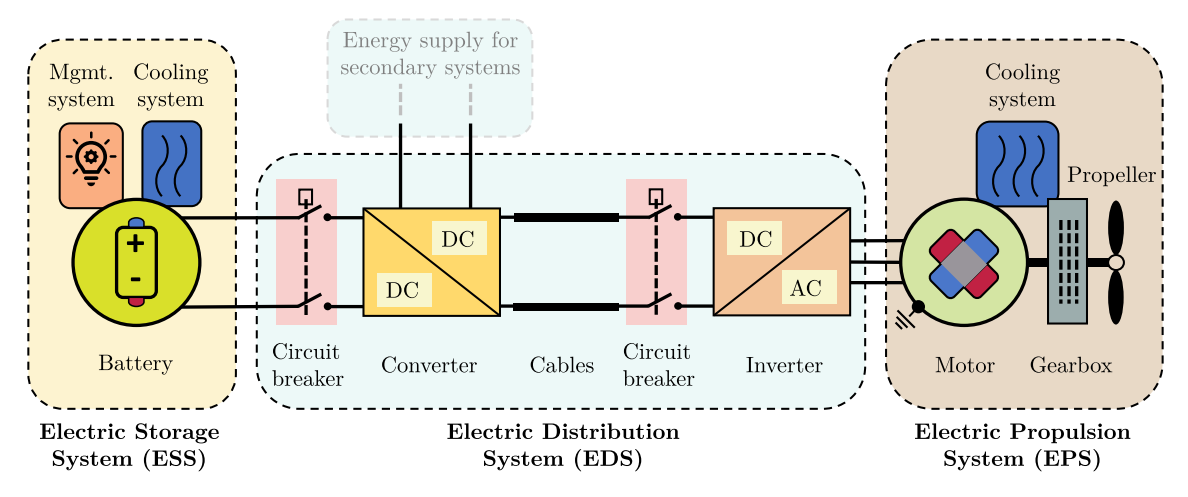


Fig. 5. Basic layout and main components of an electric drivetrain. Figure generated in orientation to Anker et al. [61].

storage system is divided into several independent battery packs [66]. In alignment with the triple-redundant design of safety-critical systems commonly applied in aviation (e.g., the hydraulic system in larger passenger aircraft [67]), we also assume installation of three redundant BMS and BCS units.

Electric Distribution System (EDS). The primary tasks of the EDS are to transmit electrical energy from the ESS to the energy consuming components and, if necessary, to adjust system voltage or current. The main components of this system are power cables and power electronics such as circuit breakers, converters, and inverters. While cables are responsible for the actual transmission through the aircraft, circuit breakers serve as protective devices. In the shown drive layout (see Fig. 5), the converter serves as an interface between the storage and the distribution system. Lastly, the inverter transforms Direct Current (DC) voltage of the distribution system into Alternating Current (AC) voltage – required for the operation of the electric motor – and additionally serves as motor control unit. Since power electronic units can produce substantial heat during operation, they need to be cooled [61]. Therefore, based on already existing aircraft, these components will be integrated into the cooling circuits for batteries and motors, respectively [68].

Electric Propulsion System (EPS). The EPS is responsible for transforming electrical energy into mechanical energy and ultimately into thrust. For that conversion, an electric motor drives a propeller, which subsequently generates propulsive force during a flight. A gearbox can be used to couple the motor's drive shaft with the propeller unit. During operation, the motor also produces large amounts of heat [69] and requires a Motor Cooling System (MCS) to avoid accelerated degradation. Since direct liquid cooling is already used for electric motors of smaller aircraft [34], we also define our MCS to be based on that approach. In addition, each motor will be cooled by its own MCS unit. For the motor itself, various studies in literature show that Permanent-Magnet Synchronous Motors (PMSMs) have the greatest potential for application in aviation due to their high specific power and efficiency [69–71].

4. Characterization of the battery systems

Due to the high purchasing costs and the anticipated strong degradation, battery cells are expected to be the predominant cost driver of the electric drive system. Consequently, we apply a degradation model to analyze the useful lifetime of the cells and to account for their influence on the total material cost. Within this chapter, we present the most significant battery parameters, an approach to size the battery storage system, and a degradation model of the battery health.

4.1. Performance and condition based parameters

The applied degradation model uses specific battery parameters that describe the operating status, the performance, and the level of degradation. The most important of these parameters are introduced in the following.

Capacity. The amount of electrical charge that the battery can store. It indicates how much electric energy a battery can supply over time and is one of the two most important characteristics for assessing a battery's performance. Due to degradation, the capacity decreases over time.

Power. The maximum amount of energy per unit time a battery can supply during operation. In general, when designing a battery system, there is a trade-off between high capacity and high power, as it is infeasible to maximize these two parameters simultaneously [72].

State of charge (SOC). The charge level of the battery can be derived from the ratio of the currently stored energy level and the maximum capacity. The value ranges between 100 %, i.e., a fully charged battery, and 0 %, i.e., a fully discharged battery.

Depth of discharge (DOD). The value, which indicates how deeply the battery is discharged within a cycle. The DOD value has the following relationship with the SOC range of a cycle:

$$DOD = SOC_{max} - SOC_{min}$$

A discharge to at least 80 % DOD is typically referred to as a deep discharge [72].

Internal resistance. The resistance, which acts in opposition to the current flow within the battery [73]. It's value is dependent on the SOC and the temperature of the battery. Due to degradation effects, the internal resistance increases over time, reducing the efficiency of the battery and the maximum available power.

4.2. Sizing of the battery systems

The battery system is sized taking into account operational boundary conditions of the flight mission. As part of this sizing process, a mission profile is defined for the AEA and HEA configurations, respectively – including the required energy and power for the corresponding flight segments. Here, the mission profile is derived from prototypical flight profiles of passenger aircraft according to the operating scenarios in Table 1, and consists of segments for standard and reserve missions. The scenario with the longest intended flight distance (917 FC/a &

Table 2 Characteristics of the battery systems, based on sizing procedure.

System	No. cells	Stored energy	Mass ¹
AEA	4,469,406	46.66 MWh	214,531 kg
HEA	321,090	3.35 MWh	15,412 kg

¹ Exclusive consideration of cell mass.

 $3.0\,\mathrm{FH/FC}$) is used for sizing the battery, whereas the world average scenario (1500 FC/a & 1.8 FH/FC) is used as a reference for the subsequent degradation analysis.

We derive the required propulsion power and the flight times of the mission segments from available literature studies [61,74–76] and scale these reference values to the use case of an electrically-driven A320 for the maximum power output. With the efficiency of the drive components, we can derive the required capacity and maximum power of the battery system. It has to be noted though, that we neglect most of the expected changes in mission profile due to an electrification of the drivetrain, e.g., changes in altitude, speed, and mass characteristics during a flight. While the overall aircraft mass decreases during a conventional mission due to the consumption of fuel, battery-powered aircraft masses remain constant – resulting in shorter ranges for equal amounts of energy [77], which is not taken into account in our analysis.

Since one of the main design requirements for battery-powered electric aircraft is to minimize the battery system mass [60], the electric drive part of the HEA configuration is designed for a power supply only during taxi and take-off. In alignment with Bien et al. [38], we further set the maximum degree of power hybridization by the electric motor to 10 % during takeoff. Additionally, besides the support in propulsion, the energy demand of the secondary systems is exclusively supplied by the battery during all flight phases.

For the definition of the battery system in our study, we assume the installation of 18650PF cells from the manufacturer Panasonic [78,79]. These are standard-sized, cylindrical Lithium-Ion Battery (LIB) cells that are already used in smaller electrically-powered aircraft [65,68,80]. Based on the methods from Ng and Datta [81] and Jäger et al. [82], we are taking the cell performance together with the required missionspecific energy and power into account to determine the battery size. Furthermore, to prevent battery cells from increased degradation due to a deep discharge [77], the last 20 % of a depleting battery charge is intended to be kept as a mission reserve. That is, the corresponding stored electrical energy should not be used during normal operation. The system voltage of the battery is set to 3 kV [83]. With these boundary conditions, the sizing process reveals that the battery size is predominantly driven by the required total energy storage and could theoretically be significantly smaller to satisfy the maximum power requirement. In general, the energy capacity is the limiting factor for longer flights, whereas the power output is the dominant factor for shorter flights [61]. The resulting characteristics of our battery system for this paper are summarized in Table 2. It has to be noted that the pack mass refers to the total mass of the individual cells without considering needed structural elements.

Considering the actual current energy density of 217.5 Wh/kg for the selected Panasonic cells, the total battery mass of the AEA configuration clearly exceeds the scope of a realistic aircraft design, as it is almost triple the Maximum Takeoff Weight (MTOW) of a conventional A320 [56]. This observation is consistent with most literature studies, which emphasize the technological challenges for large AEA with current LIBs [84], while smaller electric aircraft are also likely to experience significant limitations in their intended range and payload [60]. An increased aircraft mass will lead to a higher energy demand, which in turn increases the required capacity and mass of the battery [85]. In aircraft design, this snowball-effect can quickly result in an unfeasible concept. A potential increase in the energy density of the battery is therefore crucial for a future implementation of a battery-powered aircraft. Although energy densities are expected to increase, even an optimistic scenario of

a gravimetric energy index of 500 Wh/kg [50,86] will still be incompatible with current aircraft designs. Given these development challenges for AEA, our results still deliver valuable insights as the methodology is also applied to the far more realistic and technologically feasible HEA design concept.

When it comes to an AEA, the aircraft size should be reevaluated. Smaller regional aircraft with lower payload and range require less maximum power and energy, both of which are the basic design parameters for the required cell quantity. Our sizing process confirmed that lower energy requirements for the cruise segment of a mission in particular result in significantly reduced number of cells. Consequently, we expect a more feasible battery system for these regional aircraft in terms of size and mass

4.3. Degradation modeling of the battery cells

The degradation characteristics of battery cells are driven by numerous complex mechanisms that interact with each other and are influenced by the following factors [62,87].

- A dominant influence is the operating load due to cyclical charging and discharging, since the useful lifetime depends on the depth and frequency of these cycles. Especially for high DOD values (respectively low SOC values), a strong degradation is experienced [77].
- Operation in the medium voltage range is favorable in order to keep the degradation effects as low as possible [88].
- The operating temperature of the battery cells is also considered one
 of the main influencing factors. Battery cells experience accelerated
 aging when exceeding the temperature range of 0 °C to 50 °C [89].

The effects of cell degradation can be observed during operation by an increase in internal resistance and a decrease in capacity [87].

With the exact degradation behavior being highly dependent on the cyclical load and the specific operational conditions, using statistical failure rates from literature is not suitable for deriving replacement intervals of battery stacks. Consequently, investigations of the degradation behavior under different conditions require the application of a degradation model. There are various approaches to this, which are explained below. Complex physical models offer in-depth analyses of diverse degradation mechanisms on molecular level, but they mostly concentrate on the isolated consideration of individual aging effects and may not adequately reflect the interlinks between different effects [90]. Simpler empirical models are mainly based on experimental data and are often defined for a specific use-case scenario, while a transfer to different operating conditions may not be applicable [87]. Semi-empirical models combine physical analyses with experimental observations and are applicable to other operating conditions beyond the experimental tests [90]. As they have proven to successfully estimate battery lifetime in operational settings [91], we apply a semi-empirical degradation model established by Clarke and Alonso [89] and Schmalstieg et al. [88] in our

In order to reflect an actual operating scenario, the degradation model iterates through different flight phases, while simulating charging processes and operational pauses – taking into account battery system design parameters and flight data. Furthermore, we assume a constant operating temperature of 35 °C (measured at the surface of the battery cell), since a detailed thermal simulation of the battery system during operation would exceed the scope of this study. This assumption is based on the fact that many cell parameters used in this analysis were determined at this temperature [88]. As the model's underlying experimental tests have been conducted with a standard discharge rate [88], we keep the value fixed as well, neglecting any variation in different battery charging processes. Regarding that, two different strategies are discussed in literature – batteries can either be integrated into the aircraft and be fast-charged between two flights or modular batteries are swapped with pre-charged units [92,93]. Although both strategies have their benefits

and drawbacks, we are assuming a charging process of integrated units during turnaround in our analysis. At a more advanced stage of design, the trade-off between these charging strategies and the corresponding impact on battery maintenance should be examined in more detail.¹

Depending on (a) the performance parameters, (b) the operating temperature, and (c) the cyclic operating load of the cells, the model provides two fundamental relationships for the decrease in capacity and the increase in internal resistance. These are the decisive factors for estimating the useful lifetime of the battery cells, since they have a direct effect on the performance parameters that must be guaranteed for the execution of the flight mission. While a decreasing capacity leads to less usable energy for a mission, an increased resistance causes higher heat losses with a decreased efficiency. Consequently, at a certain threshold, the required maximum power can no longer be provided by the battery [62]. In many literature studies, a constant limit of 80 % of the initial capacity is used for determining the lifetime of batteries [76,97]. In our study, the application of this limit is considered to be too conservative, as it can potentially lead to a significant underestimation of the useful lifetime of battery cells.

In summary, a battery cell's EOL is reached once one of the following monitored conditions occurs.

Capacity-related EOL. The current capacity of the battery is insufficient to provide energy for the standard and reserve mission or the battery would be discharged below a 20 % SOC during the standard mission.

Resistance-related EOL. The available battery power is insufficient to provide the required maximum power for the mission due to the increased internal resistance.

5. Methodology of the maintenance analysis

As the level of available data differs between the electric and conventional systems, the methods for assessing the material costs also vary depending on the configuration. In all cases, the analysis is carried out in two stages. At first, with the reliability analysis, MTBF values of the components are derived that serve as an initial indication of the expected operational lifetime. In a next step, the cost analysis then links these values with the spare part prices of the components and ultimately enables the estimation of the anticipated material costs.

5.1. Reliability assessment data input

Although the reliability assessment of components can be conducted according to the three main approaches discussed in Section 2.2, we focus in our work on the empirical approach. In the case of the conventional configuration, data from real operation serve as a basis. The corresponding reliability values have been taken, among others, from the research aircraft of Deutsches Zentrum für Luft- und Raumfahrt (DLR) [98], which provides information for specific components on an LRU level. The corresponding data set contains FHs and the number of removals for each component as part of unplanned maintenance for the last 5 years. Based on this, the global fleet average MTBUR value of a component can be derived and subsequently translated into an MTBF value (see Section 2.2).

The reliability assessment of the electric drive components is conducted taking into account statistical failure rates from literature studies, as no empirical data from the actual operation is available at the moment. These values can differ significantly from each other, as they are highly dependent on the underlying loads, operational conditions,

Table 3Minimum, maximum, and mean failure rates from literature, used for the reliability analysis of the electric drivetrain.

Component	Failure rate (x10 ⁻⁶)			Ref.
	Min	Mean	Max	
BMS	1.000	1.945	5.285	[99,100]
Inverter	1.912	5.746	86.000	[50,100-108]
Converter	2.044	4.035	28.660	[106,108-110]
Circuit breaker	1.967	4.821	46.000	[47,108]
Gearbox	1.500	5.254	17.700	[111-114]
El. motor	5.930	11.330	92.400	[50,105,106]
Heat exchanger	2.863	6.170	17.300	[106,108]
Pump	12.060	19.330	59.800	[100,106,108]
Cable	0.042	0.100	0.681	[37,100,108]

and system design [51]. Even though a specific failure rate is only valid under consistent loads, operational conditions, and system design, such consistency cannot be ensured in our case due to a lack of data. Therefore, we determine average failure rates from a dataset of different failure rates from literature (see Table 3). The corresponding MTBF values are then obtained as reciprocals of those average failure rates (see Section 2.2). In order to take into account the large range between the minimum and maximum failure rates in our results, we perform an additional parameter variation with the respective extreme values in Section 6.4.1.

For the reliability assessment of the propeller units, we base the analysis on the model 568 F from *Collins Aerospace*, which is used on an Avions de Transport Régional (ATR) 42/72 aircraft [115]. Consequently, we can obtain empirical values from actual operation that show fixed overhaul intervals of 10,500 FH for the propeller blades and hub [116,117]. Lastly and in contrast to the other components of the electric drivetrain, we conduct the reliability assessment of the battery cells using the analytical approach. Since the battery's useful lifetime is limited by degradation, the EOL of the cells can be derived by applying the degradation model as described in Section 4.3. The respective results obtained from the application of the degradation model are presented in Section 6.

5.2. Cost assessment data input

First, we want to emphasize that the total material cost will result from non-routine and routine maintenance actions. Therefore, we will distinguish between these two in the following. Cost data are stated in US-\$ and historical values from literature are adjusted for inflation to the base year of 2023.

Non-routine material cost

In order to estimate the expected material costs of the conventional components, by default, we use their spare part prices as our reference. For the main engines, *Aircraft Commerce* provides a more detailed breakdown of material costs during engine shop visits for an exemplary CFM56-5B4 engine [57].

If a comparable component exists in the conventional system, its spare price data is also used for the components of the electric drive systems. This is applicable to the BMS and the sub-components of the cooling systems, in particular the pump and the heat exchanger. Data from actual operation is also used for the analysis of the propeller units, as *Aircraft Commerce* provides references for the overhaul costs of the propeller shaft and blades installed on an ATR 42/72 [116]. For all other components of the electric drive systems, actual spare part prices are not available and cost forecasts from literature are used (see Table 4).

To enable a comparison with the reference aircraft, our main cost analysis of the electric drivetrain is based on the stated values for the year 2023, which refer to the current technology and cost status in the aviation sector [118]. The cost for the battery cells is based on the average cost in the automotive sector [119], since these cells are used

¹ The trade-off between different charging strategies depends on a number of factors, such as the necessary airport infrastructure to handle the enormous charging volumes or the additional storage for the batteries [94,95]. When defining a possible charging process, it is also crucial to take into account the very stringent turnaround time requirements and the increased battery degradation caused by a high charging rate [96].

 Table 4

 Forecasts for spare part prices of the electric drivetrain.

Component	Cost	Cost			
	2023	2050	Unit		
Battery cell	112.70	64.18	\$/kWh	[119,121]	
Inverter	129.96	51.72	\$/kW	[118,120]	
Converter	129.96	51.72	\$/kW	[118,120]	
Circuit breaker	129.96	51.72	\$/kW	[118,120]	
Electric motor	63.48	20.11	\$/kW	[118,120]	
Gearbox	63.48	20.11	\$/kW	[118,120]	

as a reference in our work. However, as most of the components in Section 6.4.3 are still at a relatively low level of technological maturity in the aviation sector, major cost reductions can be expected in the coming decades. We therefore also provide an optimistic cost forecast based on the automotive industry for the year 2050 [120] and examine the respective influence on the total material costs in a parameter variation in Section $6.4.3.^2$

In the case of power electronics, the cost of the inverter or motor control unit is also used for all other components. This is considered valid, as this unit features the most complex design and it can be assumed that the costs of the power electronics will be in a similar range [122].

While the replacement of a component with a new unit usually results in material costs equivalent to the spare price, an economical repair typically reduces these costs. However, the existing reliability data does not indicate whether the removal of a component resulted in a replacement or a repair, nor does it show the associated cost for a possible repair. Therefore, to cover both cases, we define a repair-replacement-ratio factor as a reference for the average material Shop Visit Cost (SVC) – based on historical maintenance data of an A320 engine with its extensive data availability [123]. Here, the cost of a complete overhaul of an engine is set in proportion to the price of a new engine, resulting in a factor of about 21.6 %. Although this factor is applied to all component types due to a lack of maintenance data, it is consistent with engineering experience, since average maintenance cost of repairs equals about 25 % of a new component's cost [124].

Depending on (a) the spare part price $C_{\rm SparePart}$, (b) the cost factor for average material cost per shop visit $r_{\rm SVC}$, and (c) the Quantity Per Aircraft (QPA) of installed units $n_{\rm QPA}$, the material cost per LRU and FH for non-routine maintenance tasks can be calculated using Eq. (6).

$$C_{\text{LRU,non-routine}} = \frac{C_{\text{SparePart}} \cdot r_{\text{SVC}}}{t_{\text{MTDE}}} \cdot n_{\text{QPA}}$$
 (6)

with

$$r_{\text{SVC}} = 21.6 \%$$
 (7)

For the analysis of the electric drivetrains, it is assumed that the battery cells will be replaced by new units upon reaching their EOL, resulting in no battery-related repairs in our analysis. The material costs of the battery cells are determined by taking into account (a) the cost of a single cell C_{Cell} , (b) the total number of cells n_{Cells} , and (c) their useful lifetime t_{EOL} using Eq. (8).

$$C_{\text{Cells}} = \frac{C_{\text{Cell}}}{t_{\text{EOL}}} \cdot n_{\text{Cells}}$$
 (8)

In the case of the HEA configuration, additional cost adjustments resulting from hybridization must be taken into account. For the applied parallel layout, the associated decrease in operational loads of the conventional engine enables a potential cost reduction. Since the electric motor provides additional propulsive power during takeoff, the thrust of the turbofan engine can be reduced in this flight phase. Consequently, the engine components experience less severe degradation effects.³ Various studies have provided indications of this change in maintenance cost, based on a degradation analysis of an A320 engine [38–40]. In Section 6.3, we will apply these results to our use case.

Routine material cost

In addition to the material cost due to unscheduled removals, the cost counterpart for routine tasks, e.g., replacement of LLPs or other scheduled discard tasks, must also be taken into account. As these replacements are scheduled by definition, the corresponding time intervals can be retrieved from the MPD and do not have to be estimated through MTBF assessments. Furthermore, the resulting material cost equals the spare part cost since aviation regulations prohibit any repairs for these replacements. Consequently, $r_{\rm SVC}$ will be 100 % for these routine replacements, simplifying Eq. (6) to

$$C_{\text{LRU,routine}} = \frac{C_{\text{SparePart}}}{t_{\text{MTBF}}} \cdot n_{\text{QPA}} \tag{9}$$

with

$$t_{\rm MTBF} = t_{\rm MPD} \tag{10}$$

In the case of the main engines and the Auxiliary Power Unit (APU), routine material cost is not determined according to Eq. (9). Instead data from *Aircraft Commerce* is used, in which cost information for LLP replacements is provided with a higher level of detail [57,125]. In the case of electric drivetrains, there is currently no available information about the scheduled maintenance scope. For example, it is not yet clear which components will be defined as LLP or which discard tasks need to be carried out. Since this information is required for estimating the routine scope, routine material costs are not analyzed separately from the non-routine costs for the AEA and HEA configuration.

5.3. Scope of the comparative analysis

Before applying the presented methodology, we identify the systems and components that need to be considered in our comparative assessment. In the case of the conventional configuration, the scope results from the components that are affected by a change to an all-electric or hybrid-electric drive system. In our study, we use the categorization by Air Transport Association (ATA) chapters [126] to identify these components. The ATA chapters listed below serve as the basis for the analysis of the conventional systems. For consistency in the drive configuration comparison across all aircraft concepts (conventional, AEA, and HEA), we assign the individual ATA chapters to their respective sub-system, i.e., storage system, distribution system, and propulsion system. These are then compared in the analysis with the respective systems of the electric drivetrain (i.e., ESS, EDS, and EPS). It should be noted that the analysis of the HEA configuration includes parts of the conventional system as well as the electric systems.

ATA 24 – Electrical power. The electrical units and components that generate, control, and supply AC/DC electrical power for other systems [127]. In the case of electric drive systems, the basic function and structure of this chapter mainly remain unaffected. As a result, most of the components of ATA chapter 24 are not included in our comparative analysis. However, the power supply from Integrated Drive

² To meet the higher certification and performance requirements for component manufacturing in aviation, a comparison of current costs reveals an additional cost factor of approximately 2.2 [118,120]. For most components, with the exception of battery cells, we take this factor into account for projecting costs from the automotive sector to the aviation sector.

³ Hybridization results in a reduced turbine inlet temperature during takeoff. This value corresponds to the maximum temperature of the gas path, which is considered as main indicator of the degradation intensity of engine components [40]. However, beyond a power hybridization degree of about 10 %, the optimum operating range of the gas turbine is restricted, which would require changes in the design and sizing of components [38].

Table 5Primary cost drivers for routine and non-routine material costs of the conventional drive system. Averaged values per flight hour and aircraft, including all installed units.

System	Chapter	Category	Component	Cost	Unit	Share
CSS	ATA 24	Non-routine	IDG	10.57	\$/FH	4.2 %
			APU generator	1.75	\$/FH	0.7 %
			GCU	1.22	\$/FH	0.5 %
			Batteries	1.14	\$/FH	0.4 %
			Interface units	0.35	\$/FH	0.1 %
			Miscellaneous	0.03	\$/FH	0.01 %
		Routine	Filter elements	0.97	\$/FH	0.4 %
	ATA 49	Non-routine	APU engine	6.00	\$/FH	2.4 %
			APU control unit	1.20	\$/FH	0.5 %
		Routine	APU engine LLPs	3.07	\$/FH	1.2 %
			Filter elements	0.17	\$/FH	0.07 %
	Sub-total			26.46	\$/FH	10.4 %
CDS	ATA 28	Non-routine	FQIC	0.83	\$/FH	0.3 %
			Other computer units	0.30	\$/FH	0.1 %
			Miscellaneous	0.35	\$/FH	0.1 %
		Routine	-	-	-	-
	Sub-total			1.48	\$/FH	0.6 %
CPS	ATA 71–79	Non-routine	Main engines	87.04	\$/FH	34.4 %
			ECU	4.08	\$/FH	1.6 %
			TRU	3.08	\$/FH	1.2 %
			Miscellaneous	3.09	\$/FH	1.2 %
		Routine	Main engine LLPs	127.45	\$/FH	50.3 %
			Filter elements	0.70	\$/FH	0.3 %
	Sub-total			225.44	\$/FH	89.0 %
Total				253.38	\$/FH	100 %

Generators (IDGs) or the APU generator is substituted by the battery system. Consequently, these power-generating components can be removed for the AEA and HEA configuration, but need to be part of the conventional maintenance scope of our analysis in which they are assigned to the storage system.

ATA 28 – Fuel. The units and components storing and delivering fuel to the engines [127]. Components of this chapter are to be considered for the conventional as well as the HEA maintenance scope and are assigned to the distribution system. In the case of the AEA configuration, the conventional engines are replaced by electric motors and consequently all components of this chapter can be omitted.

ATA 49 – APU. All components with the purpose of generating and supplying auxiliary power, including the related control units [127]. For the electric drive configurations, the battery system is intended to fulfill the tasks of the conventional APU engine. Therefore it is assumed, that all components in this chapter can be omitted for the AEA and HEA configurations, but need to be part of the conventional maintenance scope in which they are assigned to the storage system.

ATA 71–79 – Engine. All components are dedicated to the engine and the related units [127]. Components of this chapter are part of the conventional as well as the HEA configuration and are assigned to the propulsion system, whereas they can be omitted for the AEA. We assume that the structural parts for the cowling and mounting of the engine nacelles are similar for all configurations and consequently are not part of our comparative analysis.

6. Results of the maintenance analysis

With the methodology for our analysis explained, we will present the resulting values in the following section. For each configuration, a detailed cost breakdown for the corresponding sub-systems (i.e., storage system, distribution system, and propulsion system) will be provided, followed by the total material costs. In order to evaluate the validity of the results, we will then carry out a parameter variation for the most important variables.

6.1. Conventional drive system

In the following, the material cost of the conventional system will be presented in detail. For a better comparability, we subdivide the following analysis into the Conventional Storage System (CSS), Conventional Distribution System (CDS), and Conventional Propulsion System (CPS) – with the individual ATA chapters being assigned to them. Additionally, the detailed cost breakdown of all components and systems is shown in Table 5.

Conventional Storage System (CSS)

The CSS comprises of the components for the ATA chapters 24 and 49. With a share of 94 %, the material cost of ATA chapter 24 is primarily driven by non-routine maintenance activities. IDG units have the biggest influence here, accounting for material costs of 10.57 \$/FH. Other generators, like the APU generator, or electronic computer units, such as the Generator Control Units (GCUs), additionally have a notable influence due to the considerable number of removals and their high spare part prices. The scope of routine maintenance activities is derived by the scheduled replacement of oil filter elements for the generators. Overall, ATA 24 contributes 16.03 \$/FH of material cost.

Similar to ATA 24, the material cost for ATA 49 is also primarily driven by non-routine maintenance events. With material costs of 6.00 \$/FH, the APU engine is the most substantial contributing factor here. This unit experiences a significant number of unscheduled removals due to high thermal and mechanical loads during operation [125], in addition to comparably high spare part prices. Furthermore, with 3.07 \$/FH, the APU is also a relevant cost driver when it comes to routine-maintenance-related material costs. Similar to the main engines, the APU has several sub-components that are classified as LLPs;

therefore, they must be replaced with new parts after a defined usage period. Additionally, in accordance with the MPD, the scheduled discard of oil filter elements contributes to those routine material costs. Consequently, ATA 49 contributes material costs of 10.43 \$/FH, leading to ultimate material cost per aircraft for the CSS of 26.46 \$/FH.

Conventional Distribution System (CDS)

In our comparative analysis, the CDS consists solely of the components of ATA chapter 28. The material cost of this chapter is driven entirely by non-routine maintenance actions without any routine tasks scheduled according to the MPD. Here, the main cost driver is the Fuel Quantity Indication Computer (FQIC), accounting for material costs of 0.82 \$/FH. In addition to various other computer units, this chapter consists mainly of a large number of sensors and mechanical components, e.g., valves. Since these components are usually less complex, they are characterized by high reliability values and low spare part prices. Together with the low number of components, this reliability results in comparably low average material cost for the CDS of only 1.48 \$/FH.

Conventional Propulsion System (CPS)

The CPS contains the engine-related ATA chapters 71–79. Here, the actual main engines (ATA 72) are the dominant cost drivers. According to Aircraft Commerce [57], the engines account for average material costs of 87.04 \$/FH for non-routine tasks due to performance degradation and 127.45 \$/FH for routine LLP replacements, respectively. The dominance of routine costs can be attributed to the large number of LLP units within the engine and their high associated spare prices. In addition to the main engines, the Electronic Control Unit (ECU) and the Thrust Reverser Unit (TRU) have notable influence on non-routine material costs, while the scheduled replacement of several filter elements contributes to the routine material costs. Overall, the CPS contributes average material costs of 225.44 \$/FH per aircraft.

Total cost

The considered cost components result in total material cost of the conventional drivetrain of 253.38 \$/FH per aircraft. The components of the CPS are the most relevant cost drivers with a total share of 89 %, with the main engines alone contributing about 85 % to the total cost. This dominance stems from the complex engine design, the numerous and expensive LLPs, and the high operating temperature and rotating speed ranges [57]. While components of the CSS contribute approx. 10 % to the total cost, the share of the CDS is comparatively small at less than 1 %. For the total material cost, routine maintenance activities slightly dominate with a share of 52 %, compared to 48 % for non-routine maintenance events.

6.2. All-electric drive system

In the following, the material cost of the AEA drive system will be presented in detail, with analyses of the components for the ESS, EDS, and EPS, respectively. In this section, special focus is placed on the battery system.

Electric Storage System (ESS)

The most significant cost driver for the ESS is the battery; therefore, we will analyze the results obtained from the corresponding degradation analysis first. By applying the battery degradation model, it becomes apparent that the required mission energy in conjunction with a decreasing capacity is the limiting factor for determining the EOL. Although the internal resistance increases over time as well, the required maximum power can be ensured over the whole battery lifetime. Consequently, the focus of our analysis is on the reduction of capacity depending on the battery's age and the number of charging cycles, i.e., FCs (see Fig. 6). Assuming an operating temperature of 35 °C, the battery capacity is no longer sufficient to supply the required mission energy after around 4650 FC and the cells therefore reach their EOL. This corresponds to

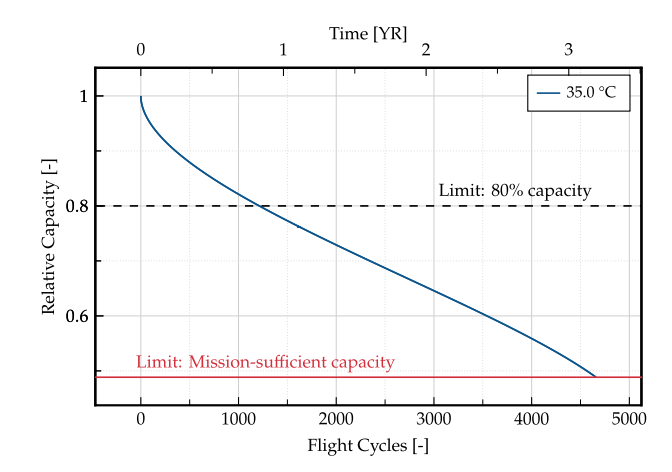


Fig. 6. Capacity fade of the AEA battery cells in relation to the initial state for an operating temperature of 35 $^{\circ}$ C.

the useful lifetime of 8370 FH with an average flight time of 1.8 FH per FC (see Table 1). However, since a prototypical capacity of 80 % is often cited as a battery's EOL, the cells would need replacement already after roughly 1200 FC or 2160 FH, respectively. Since these intervals invalidate any business case, we adhere to the mission-dependent limit rather than the limit of 80 % battery capacity as already discussed in Section 4.3.

The degradation model output is then used to determine the maintenance-related material cost of the battery cells (see Section 5.2), resulting in 627.15 \$/FH. In addition to the battery cells, the ESS also contains BCS units, i.e., cooling systems consisting of pumps, heat exchangers, and piping. By applying Eq. (6), we estimate their corresponding material costs to equal 1.66 \$/FH. The spare part prices and failure rates of the BCS units are determined as the sum of the respective values of the sub-components. Following the approach of Birolini [49] for determining the failure rate of a system consisting of multiple units, it is assumed that all sub-components are necessary to perform the required system function. It should be noted that the impact of the piping is neglected, since these are rather simple structural elements with high reliability and low spare part prices. Lastly, the costs of the required BMS units also hardly contribute to the total cost. Although costly when replaced, these components have comparatively high reliability values (see Section 5.1) so that their replacement intervals are rather long. With these contributors factored in, we expect the overall average material cost for the ESS to equal 628.89 \$/FH.

Electric Distribution System (EDS)

The EDS mainly consists of various power electronics with comparable spare part prices and reliability values (see Section 5.1 and Section 5.2). With estimated material cost contributions of 6.43 \$/FH, the circuit breakers are the main cost contributors in this system — mainly because of the high number of units needed for the electric drivetrain. Additionally, while the material costs of inverters are expected to amount to 3.73 \$/FH, converters account for costs of 2.68 \$/FH. This difference can be attributed to the slightly lower reliability of the inverter which serves as a control unit of the electric motor and is potentially more complex in its design. Lastly, the associated costs of the cable system and other connecting elements are considered to be comparatively low [30]. With their extremely low failure rates, we have not included these components in our analysis. Consequently, the average material cost of the EDS results in 12.84 \$/FH.

Electric Propulsion System (EPS)

The material cost of the EPS is predominantly driven by the propeller units with expected costs of 16.41 \$/FH - mainly caused by

Table 6Total material cost for the AEA drive system. Averaged values per flight hour and aircraft, including all installed units.

System	Component	Cost	Unit	Share
ESS	Battery cells	627.15	\$/FH	94.2 %
	BCS	1.66	\$/FH	0.2 %
	BMS	0.08	\$/FH	0.01 %
	Sub-total	628.89	\$/FH	94.5 %
EDS	Circuit breakers	6.43	\$/FH	1.0 %
	Inverters	3.73	\$/FH	0.6 %
	Converters	2.68	\$/FH	0.4 %
	Sub-total	12.84	\$/FH	1.9 %
EPS	Propeller units	16.41	\$/FH	2.4 %
	Electric motors	3.52	\$/FH	0.5 %
	MCS	2.21	\$/FH	0.3 %
	Gearboxes	1.62	\$/FH	0.2 %
	Sub-total	23.76	\$/FH	3.6 %
Total	-	665.49	\$/FH	100 %

fixed overhauls of the propeller hub and blades due to corroding effects [116]. Additionally, the electric motors contribute material costs of 3.52 \$/FH. For these rotating machines, maintenance activities are typically caused by aging effects on the insulation system and mechanical loads on the bearings [69,128]. Lastly, MCS units and gearboxes contribute 2.21 \$/FH and 1.62 \$/FH, respectively, to the cost of the EPS, resulting in the overall expected material cost of 23.76 \$/FH for this system.

Total cost

The material costs for all relevant units of an AEA drivetrain are shown in Table 6 and amount to a total cost of 665.49 \$/FH per aircraft. Here, with a share of about 94 %, the ESS is clearly the most significant cost contributor, which is almost entirely attributable to the battery cells. Compared to the ESS, the EDS with a share of approx. 2 % and the EPS with roughly 4 % have hardly any influence on the overall cost. For these two systems, the propeller units account for the largest cost contribution. The differences in cost share among the sub-systems can mainly be attributed to the comparatively low spare part prices and high reliability values of the EDS and EPS components. However, it should be noted that the reliability analysis of the battery cells with its degradation model tends to have fewer uncertainties and be more realistic compared to the statistical MTBF-value-based reliability assessment of other components. In particular, it is difficult to consider all operating conditions with their impact on degradation and the resulting MTBF values. For a more accurate analysis, this consideration would be essential for lifetime estimations; for example, the degradation intensity of power electronics highly depends on their operating temperature and voltage [50]. To assess the validity of the MTBF values, we perform a simplified parameter variation in Section 6.4.1.

6.3. Hybrid-electric drive system

The HEA configuration consists of conventional and electric drivetrain components, combined as the joint Hybrid Storage System (HSS), Hybrid Distribution System (HDS), and Hybrid Propulsion System (HPS). Consequently, the analysis is based on the results of Section 6.1 and Section 6.2, which are adjusted for this use case.

Hybrid Storage System (HSS)

The HEA configuration is characterized by the substitution of conventional power-generating components with a battery system. Therefore, we expect no conventional components to be part of the HSS. For the electric part, the costs of the battery cells are again determined based on their useful lifetime. For this purpose, we apply the degradation

model with the specifications of the HEA battery sizing and mission profiles (see Section 4.2). With this information, the mission-specific EOL is expected to be reached at roughly 2150 FC or 3870 FH, resulting in material costs of 96.91 \$/FH for the cells. Due to the significantly smaller batteries and lower cyclical loads, the costs of the HEA batteries are reduced by approx. 85 % compared to the AEA configuration. With respect to the AEA analysis, the material costs of the BCS and BMS units remain unchanged, as these are determined independently from the battery system size. Ultimately, we estimate the overall average material cost of the combined HSS to equal 98.65 \$/FH.

Hybrid Distribution System (HDS)

The HDS consists of both conventional and electric components. As the main engines still need to be supplied with fuel, the material cost of the conventional part of the system remains at 1.48 \$/FH. The layout of the electric part of the system is based on the AEA configuration, consisting of the same components. However, they have to deliver significantly less power; therefore, these components result in considerably lower spare part prices (see Table 4). This reduction translates in material cost of 1.24 \$/FH for the electric part, delivering combined material cost of 2.72 \$/FH.

Hybrid Propulsion System (HPS)

The HPS also consists of a conventional and electric part. As shown in Section 5.2, the hybridization impacts the operation and degradation intensity of the conventional engine. According to Bien et al. [38], a degree of hybridization of 10 % can reduce an engine's DMC per shop visit by about 11 %. In our analysis, these results are applied to the non-routine engine cost, reducing the corresponding conventional cost of 87.04 \$/FH to 77.45 \$/FH. For the routine cost components (i.e., engine LLPs), their operational life is not only affected by the turbine inlet temperature during takeoff but predominantly by time-based life consumption [38]. Therefore, it would require more complex analyses to derive the effects of hybridization on routine maintenance costs. As a simplification, we assume the routine material cost for the engine to stay unchanged at 127.45 \$/FH. In addition, material costs of the ECUs, the TRUs, and miscellaneous components (including the routine costs of filter elements) need to be considered, which results in overall material cost of 215.86 \$/FH for the conventional part of the HPS system. Besides the conventional components, the material costs of the electric part of the system must be taken into account, which are significantly lower at 1.6 \$/FH. Similar to the HDS, these values have also been scaled down by the reduction of required power output (see Table 4). Ultimately, with these adjustments, the overall material cost of the combined HPS then results in 217.46 \$/FH.

Total cost

The final cost breakdown for all components of the HEA drivetrain is shown in Table 7, amounting to 318.83 \$/FH in total. The main contributor to these costs is the HPS with a share of roughly 68 %. Even though hybridization can reduce the material costs for the conventional engines, they still remain the biggest cost driver, accounting for almost 2/3 of the total cost. With a share of approx. 31 %, the HSS has the second largest impact in terms of cost, being almost entirely attributable to the battery cells. In comparison, the components of the HDS hardly impact the total cost at all.

6.4. Parameter variations and their cost effects

With the unavailability of actual operational data for electric drive systems, our analysis in this study is subject to uncertainties. In order to gather some insights into the accuracy of our results and to account for exemplary uncertainty factors, we want to conduct a simplified parameter variation. Specifically, we want to examine the effects of different failure intervals, the variation of selected battery parameters, and higher technological component maturity on the resulting material cost of the AEA drive system.

Table 7Total material cost for the HEA drive system. Averaged values per flight hour and aircraft, including all installed units.

System	Drivetrain	Component	Cost	Unit	Share
HSS	Conventional	-	-	-	-
	Electric	Battery cells	96.91	\$/FH	30.4 %
		BCS	1.66	\$/FH	0.5 %
		BMS	0.08	\$/FH	0.03 %
	Sub-total		98.65	\$/FH	30.9 %
HDS	Conventional	FQIC	0.83	\$/FH	0.3 %
		Miscellaneous	0.65	\$/FH	0.2 %
	Electric	Circuit breakers	0.62	\$/FH	0.2 %
		Inverters	0.36	\$/FH	0.1 %
		Converters	0.26	\$/FH	0.1 %
	Sub-total		2.72	\$/FH	0.9 %
HPS	Conventional	Main engines	204.91	\$/FH	64.3 %
		ECU	4.08	\$/FH	1.3 %
		TRU	3.08	\$/FH	1.0 %
		Miscellaneous	3.79	\$/FH	1.2 %
	Electric	MCS	1.11	\$/FH	0.3 %
		Electric motors	0.34	\$/FH	0.1 %
		Gearboxes	0.15	\$/FH	0.05 %
	Sub-total		217.46	\$/FH	68.2 %
Total			318.83	\$/FH	100 %

6.4.1. Variation of the failure interval

As described in Section 5.1, the repair or replacement interval for most of the electric drive components is estimated based on the components' reliability, which is derived by taking into account various failure rates from literature. This methodology has two major uncertainty factors, namely the range of the failure rates and the underlying failure probability. In the following, we examine the impact of these uncertainties on the final results. We want to emphasize that the estimated material cost for the battery cells and propeller units is not affected by the adjusted interval, since their reliability analysis is not based on MTBF values (see Section 5.1).

Examination of minimum and maximum failure rates. Table 3 lists the minimum, maximum, and average failure rates of the components, derived from literature studies. A comparison of the values shows that the range of data and, consequently, the uncertainty of the calculated average failure rates is significant. To consider the impact of this range, we examine two reliability scenarios: An optimistic assessment with minimum failure rates and a pessimistic assessment based on the maximum values. The optimistic estimate results in a total material cost for the AEA drive system of 653.41 \$/FH, corresponding to a relative decrease of roughly -2 % compared to the base analysis that takes into account the average failure rates. By contrast, the pessimistic estimate results in 826.00 \$/FH (+24 %). These results and the list of failure rates indicate that the average failure rates tend to be in the region of the minimum values, while they can deviate widely from the maximum values in some cases. In the pessimistic scenario, this leads to significantly higher material costs, particularly for the electric motor and power electronics (inverter, converter, and circuit breaker).

Adjustment of the failure probability. With the expected value of the failure probability being considered as the average lifetime of components, MTBF values are usually used for reliability assessments. Even though the MTBF information is used for estimating intervals of maintenance tasks in our study, these values should generally not be misunderstood as repair frequencies or operating times without failures. The MTBF is first and foremost a measurement of failure probabilities. These probabilities are based on a certain distribution, with the expected value (i.e., the distribution's average) equaling the MTBF. Since we assume a constant failure rate for our components (see Section 2.2), i.e., there are no

dominating effects of "infant mortality failures" nor wear-out failures, the failure probability can be estimated with an exponential distribution [49]. For this distribution, the expected value (our MTBF) represents the time when there is a 63.2 % probability that an item will experience a failure [51]. Therefore, in terms of our analysis, this MTBF information translates to expected maintenance (i.e., repair or part replacement) when 63.2 % of all units in service would have experienced a failure already.

However, if the maintenance activities are to be based on a failure probability of 50 %, the nature of MTBF information, as seen before, would lead to an overestimation of time intervals. The time when there is a 50 % probability that the item will experience a failure can be determined by the median of the distribution, which can be calculated for an exponential distribution as shown in Eq. (11).

$$t_{\text{MTBF,50}\%} = \frac{ln(2)}{\lambda} \tag{11}$$

By applying this adjusted interval, the total material cost of the AEA drive system increases from 665.49 \$/FH to 675.22 \$/FH per aircraft, corresponding to a relative increase of roughly 2 %. Therefore, we can demonstrate that a statistical adjustment of the original MTBF definition has hardly any influence on the overall material cost. Consequently, despite common scepticism regarding the estimation of maintenance intervals based on MTBF values, their application for the purpose of a cost assessment appears to be viable.

6.4.2. Variation of battery parameters

The useful lifetime of battery cells, estimated through application of a degradation model, is highly dependent on certain operating conditions of the battery – predominantly the operational load and the operating temperature. As these conditions for an AEA are not yet fully specified, this section is dedicated to examining the effects of a variation of these parameters on the resulting costs. Based on these results, we derive specific recommendations for an optimized battery operation in terms of maintenance costs in Section 7.

Changes in operational load. In the previous sections, the utilization factors of a world-average flight scenario (see Table 1) were used as a reference for the application of the battery degradation model. Since the battery systems were sized according to the required energy of the

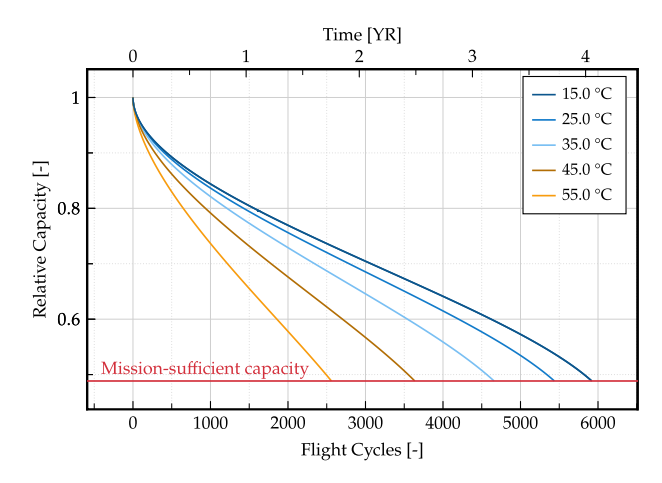


Fig. 7. Capacity fade of the AEA battery cells in relation to the initial state for different operating temperatures.

longest intended flight, the battery is significantly oversized for carrying out the average mission and can still provide sufficient energy, even after a substantial fade in capacity. If we change the underlying mission scenario to allow longer flight segments, corresponding to the long-flight-segments scenario of Table 1, the capacity fade leads to a much earlier battery EOL. In addition, we expect the cells to experience higher DODs during the mission, causing higher degradation rates. With these settings, the battery cells achieve a useful lifetime of merely 285 FC or 856 FH, respectively. Compared to the average flight scenario from before, this corresponds to a reduction in useful lifetime of about 90 %. Consequently, the total material cost of the AEA drive system would skyrocket to 6182.58 \$/FH, rendering such a use as economically impossible with current battery technologies.

Changes in operating temperature. In order to assess the influence of the battery operating temperature on its useful lifetime, we examined four additional use cases with temperatures ranging between 15 °C and 55 °C. The corresponding capacity fade curves for the battery cells of the AEA system are shown in Fig. 7. While battery cells with an operating temperature of 15 °C reach their EOL at about 5920 FC (+27 % compared to the reference temperature of 35 °C), cells that are subjected to temperatures of 55 °C only last about 2560 FC (-45 %) before their capacity becomes insufficient to complete the intended aircraft mission. These changes result in total material costs for the AEA drive system of 531.92 \$/FH (-20 %) for 15 °C and 1179.48 \$/FH (+77 %) for 55 °C, respectively.

6.4.3. Variations in technological maturity and spare part costs

Since most of the components of the electric drivetrain are not yet commercially available in the aviation sector, spare part price assumptions are subject to significant uncertainties. The impact of a more advanced stage of technological maturity on spare part prices is addressed in our work through a forecast for the year 2050 (see Table 4). By applying the aforementioned cost prognosis to our analysis, the total material cost of the AEA drive system is reduced from 665.49 \$/FH to 384.18 \$/FH per aircraft. The corresponding relative decline of approx. –42 % is mainly attributable to the impact of lower battery cell costs, which in this case amount to 357.07 \$/FH, while the remaining portion is attributable to the other components of Table 4.

In addition to LIBs, other battery technologies that are not currently considered technologically viable could also become relevant by the year 2050. Solid-state, lithium-sulfur, and lithium-air batteries are discussed extensively in literature, as they offer higher theoretical energy densities [70,129,130]. The prognosis from Mauler at al. [121] identified the lithium-air technology as having the lowest expected cost by 2050,

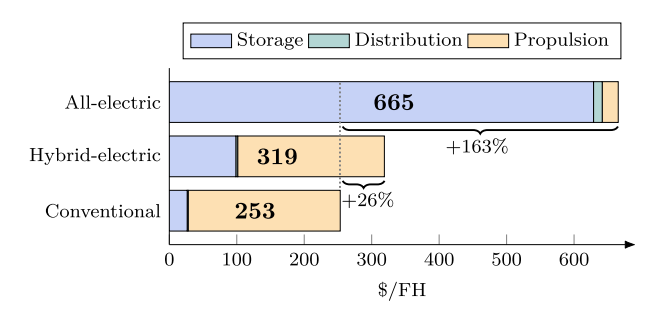


Fig. 8. Comparison of the average material cost per aircraft for the investigated drive configurations, highlighting the share of the Storage, Distribution, and Propulsion Systems.

with 53.48 \$/kWh on cell level. Assuming a lithium-air battery in our study and applying this cost improvement, the total material cost of the AEA drive system amount to 297.56 \$/FH, corresponding to a relative decrease of roughly -55 % compared to the base year 2023 and conventional LIB technologies. The useful lifetime of the battery was not varied in this case, as there are no clear indications in the literature yet on how this will change for a fully developed lithium-air battery [70,131,132].

7. Conclusion of the study

Although all operating costs must be taken into account for a comprehensive assessment, the analysis in our study already allows a first evaluation of the cost efficiency of the selected drive systems from a maintenance perspective. As shown in Fig. 8, maintenance-related material costs are expected to increase by approx. 163 % for all-electric and by 26 % for hybrid-electric aircraft configurations. In addition to the economic challenges, we also want to highlight the expected technological obstacles of the AEA configuration in terms of battery mass (see Section 4.2). Considering the current energy density of LIB technology, the cells alone would almost triple the MTOW of an A320 for comparable mission requirements. In contrast to that, the HEA configuration of this aircraft type shows great potential for an early adoption, from both a monetary and technology perspective.

Our cost estimations are based on the current state of technology and significant cost improvements can be expected taking into account new technologies, such as lithium-air batteries. For a 2050 forecast horizon, the material cost of an AEA could decrease by -55 % compared to an all-electric system based on current technology, making implementation much more feasible (see Section 6.4.3). Despite the electrification of smaller regional aircraft involving fewer challenges from an economic and technological perspective (e.g., lower maintenance costs and reduced battery mass), we expect the trends and main cost drivers discussed in the following section to apply to these aircraft types as well.

Looking at the cost distribution for an electric drivetrain, the main cost drivers are shifting from the propulsion engine to the storage system. While 85 % of material cost of the conventional system is driven by the components of the turbofan engine, battery cells are responsible for 94 % of the material cost for an AEA counterpart. This is mainly due to the enormous number of cells required for an AEA of this size, which results in high spare part prices for replacing battery packs once they reach their EOL. At the same time, strong degradation effects of the cells shorten their useful lifespan. Therefore, with the aspects shown in Section 5.1, battery cells have significantly shorter replacement intervals compared to other components. Furthermore, due to the chemical structure of the cells, it is also not possible to perform conventional repairs, which could substantially lower the material cost. We want to note though that some materials can be recycled after their replacement [133]. In contrast to the conventional configuration, components of the AEA propulsion system have only a minor impact on the total cost. This can mainly be attributed to the fact that electric motors are significantly

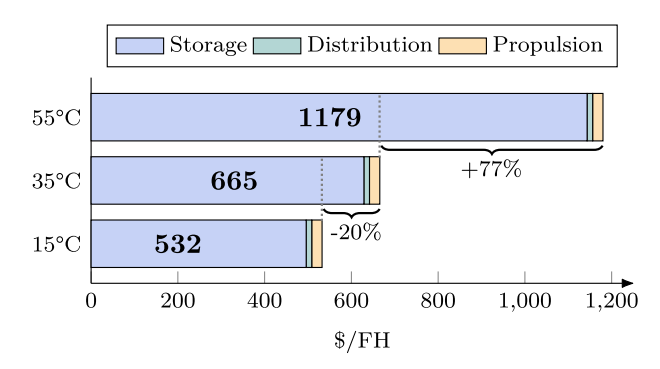


Fig. 9. Comparison of the average material cost per aircraft for the AEA configuration, analyzing the impact of different operating temperatures of the battery system.

less vulnerable to failure than turbofan engines due to their smaller number of moving components [50] and lower spare parts prices.

Due to its major impact, a cost-optimized battery system is of crucial importance. Our results highlight an important recommendation for future battery development: The focus should not solely be on optimizing specific energy densities, but also on improving the battery's service life by reducing its susceptibility to degradation. At the same time, maintenance-related material costs can be minimized by levers in battery design and operation. Based on our results in Section 6.4.2, we can derive specific operating and design recommendations. Simulating battery degradation for a long flight segment of 3 FH per FC will reduce the useful lifetime of the cells by approx. 90 % compared to an average mission length of only 1.8 FH per FC. This highlights the importance of high capacity reserves with over-sized batteries, automatically resulting in lower DODs during flight missions and reducing degradation. Although an over-sizing increases the number of cells and the cost for a system replacement, these reduced degradation effects enable significantly extended replacement intervals, resulting in lower overall material costs per flight hour. It has to be noted though, that unrestricted over-sizing of the battery is limited by mass-specific constraints of the drive system that must be taken into account.

For the battery's operating temperature, the relative changes as well as the capacity fade curves in Fig. 7 imply that variations in the higher temperature range tend to have a greater influence on the useful lifetime than variations of the same magnitude in the lower range. Fig. 9 shows the respective effects on the total material cost of the AEA drivetrain. Accordingly, an increase in operating temperature of 20 °C results in a cost increase of approx. 77 %, whereas a corresponding decrease in temperature leads to a reduction in material cost of approx. 20 %. Therefore, in order to prevent severe degradation effects, high temperature ranges should strictly be avoided during battery operation. To reduce the requirements of the temperature management, we propose that the system should not necessarily be designed to maintain the operating temperature at an exact value, but rather ensure operation within an acceptable temperature range. This seems appropriate, since changes in useful lifetime do not appear to be significant within low-temperature ranges.

Another focus of our study is the impact of hybridization on maintenance costs, which was analyzed for the HEA configuration in Section 6.4.2. Here, we assumed a maximum degree of power hybridization of 10 % during takeoff. Due to the lower degradation of the main engines and the elimination of some power-generating components, this hybridization enables a reduction in material costs of 36.05 \$/FH for the conventional part of the drivetrain. However, these savings are not sufficient to compensate for the material costs of the additional components of the electric drivetrain that amount to 101.49 \$/FH. We can observe that an increase in the hybridization degree has a substantial positive impact on the material costs of the conventional drivetrain, as

it results in lower degradation of the conventional engine. This effect is also greater than the slight cost increase due to the higher performance demand for the electric drivetrain components. Since the battery only supplies the drivetrain during the comparably short takeoff phase, it can deliver a high power without significantly increasing the required number of cells and system mass. This observation can also be attributed to the fact that the maximum power is not the limiting factor for the sizing process of our battery system (see Section 4.2).

Based on this study, we can identify the following three key findings, referring to the research objectives outlined in the introduction of our work

- F₁ Due to an increase in material costs of 163 %, a fully battery-powered A320-equivalent does not appear to be economically viable from a maintenance perspective. With a more manageable increase of only 26 %, a hybrid-electric A320-equivalent seems to offer a significantly higher potential for a quicker market entry. Furthermore, cost-optimizing decisions should focus on the design and operation of the battery system, as this is by far the greatest cost driver.
- F₂ In order to optimize maintenance costs, the battery system should be over-sized by a certain reserve capacity. A trade-off has to be established in aircraft design, since this contradicts the common goal of low battery mass. Furthermore, high operating temperatures should be avoided to minimize degradation.
- F₃ The parallel hybrid configuration enables a high degree of hybridization during takeoff; therefore, it reduces the degradation of the turbofan engine without a major increase in battery mass.

As we had to limit the complexity for the scope of this paper, the analysis is subject to a number of limitations as listed below.

- L₁ The derivation of maintenance intervals based on MTBF values is subject to certain constraints. Apart from the battery cells, specific operating conditions were not taken into account. Consequently, the results should be considered as statistical indicators that are valid at the average fleet level but may vary between different aircraft or individual components.
- L₂ Due to the limited data available, a constant factor is applied to all components in order to account for a repair-replacementratio. However, the repair characteristics may vary depending on the component type and should be adjusted for more in-depth analyses.
- ${
 m L}_3$ As no real components can currently serve as a reference, assumptions were made for the electric drive configurations, e.g., the forecast of spare part prices.

8. Summary and outlook

In this work, we have examined how spare part demand and the resulting material cost due to unavoidable degradation can be expected to change for battery-powered drive systems compared to kerosene-powered conventional systems.

By defining an all-electric and a hybrid-electric configuration on the basis of an Airbus A320 and subjecting the components to a reliability and cost analysis, we carried out a preliminary assessment of maintenance cost efficiencies for these systems. With this comparative study, we have demonstrated that a battery-powered all-electric aircraft in this size clearly exceeds the scope of an economically viable concept from a maintenance perspective, as an increase in material cost of approx. 163 % is to be expected. At the same time, we have highlighted the potential of the hybrid-electric configuration, where an increase of approx. 26 % seems manageable. Thus, this work provides a clear indication of the preferable hybrid-electric concept for this size category and in accordance with maintenance-related criteria.

As battery cells have proven to be the main cost driver, a particular focus of our work has been on analyzing these components. After sizing

the battery systems, a semi-empirical degradation model has been applied, for which we have developed an approach to estimate the useful lifetime of the battery cells depending on the specific mission requirements. By conducting a parameter variation, we have identified specific recommendations to minimize maintenance-related costs. The level of over-sizing and the operating temperature of the cells are particularly important design and operating criteria here. In order to realize larger battery-powered aircraft, future battery developments should focus on improving the service life by reducing the susceptibility to degradation.

Furthermore, we have investigated the trade-off in hybrid-electric aircraft design, evaluating cost savings for the conventional engine and additional material costs for the electric drivetrain depending on the degree of hybridization. Although the additional costs of the electric drivetrain dominate, the configuration has shown great potential, as in theory a high degree of hybridization can be achieved during take-off without significantly increasing the battery mass. Our investigation closes a relevant research gap, as conventional and electric drivetrains of a hybrid configuration have not yet been investigated jointly with regard to the degradation-based material cost.

Overall, the approach developed in our work shows great potential to be integrated into a holistic assessment of the cost efficiency of an aircraft in an early design stage. In order to cover all relevant drivers of direct maintenance costs, future studies should address the labor scope in maintenance of electric drivetrains, with a particular focus on routine tasks. Furthermore, the analysis in this work can be extended to off-wing maintenance or applied to other propulsion concepts, e.g., hydrogen-based systems. In doing so, the limitations outlined in this paper should be addressed.

CRediT authorship contribution statement

Jan-Alexander Wolf: Writing – original draft, Visualization, Methodology, Formal analysis, Data curation, Conceptualization. Robert Meissner: Writing – review & editing, Visualization, Methodology, Conceptualization. Ahmad Ali Pohya: Writing – review & editing, Project administration. Gerko Wende: Supervision, Funding acquisition.

Declaration of competing interest

The authors declare that they have no known competing financial interests or personal relationships that could have appeared to influence the work reported in this paper.

Data availability

Data will be made available on request.

References

- [1] Barke, A., Thies, C., Melo, S.P., Cerdas, F., Herrmann, C., Spengler, T.S. Maintenance, repair, and overhaul of aircraft with novel propulsion concepts analysis of environmental and economic impacts. Procedia CIRP 2023:116:221–226. https://doi.org/10.1016/j.procir.2023.02.038.
- [2] Terrenoire, E., Hauglustaine, D.A., Gasser, T., Penanhoat, O. The contribution of carbon dioxide emissions from the aviation sector to future climate change. Environmental Research Letters 2019;14(8):084019. https://doi.org/10.1088/ 1748-9326/ab3086.
- [3] Adler, E.J., Martins, J.R. Hydrogen-powered aircraft: Fundamental concepts, key technologies, and environmental impacts. Progress in Aerospace Sciences 2023;141:100922. https://doi.org/10.1016/j.paerosci.2023.100922.
- [4] Rahn, A., Dahlmann, K., Linke, F., Kühlen, M., Sprecher, B., Dransfeld, C., Wende, G. Quantifying climate impacts of flight operations: A discrete-event life cycle assessment approach. Transportation Research Part D: Transport and Environment 2025;141:104646. https://doi.org/10.1016/j.trd.2025.104646.
- [5] European Commission: Directorate-General for Research and Innovation. Fly the green deal – europe's vision for sustainable aviation. 2022. https://op.europa.eu/en/publication-detail/-/publication/69dfdaf4-07d5-11ed-acce-01aa75ed71a1. https://doi.org/10.2777/732726.
- [6] Graham, W.R., Hall, C.A., Vera Morales, M. The potential of future aircraft technology for noise and pollutant emissions reduction. Transport Policy 2014;34:36–51. https://doi.org/10.1016/j.tranpol.2014.02.017.

- [7] Barbosa, F.C. Ultra high bypass ratio engine technology review the efficiency frontier for the turbofanpropulsion. SAE Technical Paper Series 2021;https://doi. org/10.4271/2021-36-0032.
- [8] Pornet, C. Electric drives for propulsion system of transport aircraft. In: Chomat, M., ed. New Applications of Electric Drives. InTech. ISBN 978-953-51-2233-3; 2015: 115-140. https://doi.org/10.5772/61506.
- [9] Wang, B., Ting, Z.J., Zhao, M. Sustainable aviation fuels: Key opportunities and challenges in lowering carbon emissions for aviation industry. Carbon Capture Science & Technology 2024;13:100263. https://doi.org/10.1016/j.ccst. 2024.100263.
- [10] Ramm, J., Rahn, A., Silberhorn, D., Wicke, K., Wende, G., Papantoni, V., Linke, F., Kühlen, M., Dahlmann, K. Assessing the feasibility of hydrogen-powered aircraft: A comparative economic and environmental analysis. Journal of Aircraft 2024;61(5):1337–1353. https://doi.org/10.2514/1.C037463.
- [11] Renouard-Vallet, G., Saballus, M., Schmithals, G., Schirmer, J., Kallo, J., Friedrich, K.A. Improving the environmental impact of civil aircraft by fuel cell technology: concepts and technological progress. Energy & Environmental Science 2010;3(10):1458. https://doi.org/10.1039/b925930a.
- [12] Baumeister, S., Krstić Simić, T., Ganić, E. Emissions reduction potentials in business aviation with electric aircraft. Transportation Research Part D: Transport and Environment 2024;136:104415. https://doi.org/10.1016/j.trd.2024.104415.
- [13] Gnadt, A.R., Speth, R.L., Sabnis, J.S., Barrett, S.R. Technical and environmental assessment of all-electric 180-passenger commercial aircraft. Progress in Aerospace Sciences 2019;105:1–30. https://doi.org/10.1016/j.paerosci.2018.11.002.
- [14] Meissner, R., Sieb, P., Wollenhaupt, E., Haberkorn, S., Wicke, K., Wende, G. Towards climate-neutral aviation: Assessment of maintenance requirements for airborne hydrogen storage and distribution systems. International Journal of Hydrogen Energy 2023;48(75):29367–29390. https://doi.org/10.1016/j.ijhydene. 2023.04.058.
- [15] Eaton, J., Naraghi, M., Boyd, J.G. Regional pathways for all-electric aircraft to reduce aviation sector greenhouse gas emissions. Applied Energy 2024;373:123831. https://doi.org/10.1016/j.apenergy.2024.123831.
- [16] Gao, L., Jiang, Z., Dougal, R.A. An actively controlled fuel cell/battery hybrid to meet pulsed power demands. Journal of Power Sources 2004;130(1-2):202–207. https://doi.org/10.1016/j.jpowsour.2003.12.052.
- [17] Pellow, M.A., Emmott, C.J.M., Barnhart, C.J., Benson, S.M. Hydrogen or batteries for grid storage? a net energy analysis. Energy & Environmental Science 2015;8(7):1938–1952. https://doi.org/10.1039/C4EE04041D.
- [18] Gray, N., O'Shea, R., Wall, D., Smyth, B., Lens, P.N., Murphy, J.D. Batteries, fuel cells, or engines? a probabilistic economic and environmental assessment of electricity and electrofuels for heavy goods vehicles. Advances in Applied Energy 2022;8:100110. https://doi.org/10.1016/j.adapen.2022.100110.
- [19] Tsakiris, A. Analysis of hydrogen fuel cell and battery efficiency. World Sustainable Energy Days - Young Energy Researchers Conference 2019.
- [20] Prussi, M., Noussan, M., Laveneziana, L., Chiaramonti, D. The risk of increasing energy demand while pursuing decarbonisation: the case of the e-fuels for the eu aviation sector. Transport Policy 2025;160:154–158. https://doi.org/10.1016/ j.tranpol.2024.11.007.
- [21] Moebs, N., Eisenhut, D., Windels, E., van der Pols, J., Strohmayer, A. Adaptive initial sizing method and safety assessment for hybrid-electric regional aircraft. Aerospace 2022;9(3):150. https://doi.org/10.3390/aerospace9030150.
- [22] Goldberg, C., Nalianda, D., Sethi, V., Pilidis, P., Singh, R., Kyprianidis, K. Assessment of an energy-efficient aircraft concept from a techno-economic perspective. Applied Energy 2018;221:229–238. https://doi.org/10.1016/j.apenergy.2018.03.163.
- [23] Hoff, T., Becker, F., Dadashi, A., Wicke, K., Wende, G. Implementation of fuel cells in aviation from a maintenance, repair and overhaul perspective. Aerospace 2023;10(1):23. https://doi.org/10.3390/aerospace10010023.
- [24] Hölzel, N. Ein bewertungsansatz zur analyse von zustandsmanagementsystemen in verkehrsflugzeugen unter berücksichtigung neuer instandhaltungskonzepte. Ph.D. thesis; DLR; 2019. https://doi.org/10.15480/882.2543.
- [25] Gu, J., Zhang, G., Li, K. Efficient aircraft spare parts inventory management under demand uncertainty. Journal of Air Transport Management 2015;(42):101–109.
- [26] Zhang, Q., Chung, S.H., Ma, H.L., Sun, X. Robust aircraft maintenance routing with heterogeneous aircraft maintenance tasks. Transportation Research Part C: Emerging Technologies 2024;160:104518. https://doi.org/10.1016/j.trc.2024.
- [27] Curran, R., Raghunathan, S., Price, M. Review of aerospace engineering cost modelling: The genetic causal approach. Progress in Aerospace Sciences 2004;40(8):487–534. https://doi.org/10.1016/j.paerosci.2004.10.001.
- [28] Fioriti, M., Vercella, V., Viola, N. Cost-estimating model for aircraft maintenance. Journal of Aircraft 2018;55(4):1564–1575. https://doi.org/10.2514/1.C034664.
- [29] Wehrspohn, J., Rahn, A., Papantoni, V., Silberhorn, D., Burschyk, T., Schröder, M., Linke, F., Dahlmann, K., Kühlen, M., Wicke, K., Wende, G. A detailed and comparative economic analysis of hybrid-electric aircraft concepts considering environmental assessment factors. AIAA AVIATION 2022 Forum 2022;https://doi.org/10.2514/6.2022-3882.
- [30] Finger, F., Goetten, F., Braun, C., Bil, C. Cost estimation methods for hybrid-electric general aviation aircraft. ASIA Pacific International Symposium on Aerospace Technology 2019; https://www.researchgate.net/publication/337757069.
- [31] Monjon, M.M., Freire, C.M. Conceptual design and operating costs evaluation of a 19-seat all-electric aircraft for regional aviation. AIAA Propulsion and Energy 2020 Forum 2020;https://doi.org/10.2514/6.2020-3591.

- [32] Schäfer, A.W., Barrett, S.R.H., Doyme, K., Dray, L.M., Gnadt, A.R., Self, R., O'Sullivan, A., Synodinos, A.P., Torija, A.J. Technological, economic and environmental prospects of all-electric aircraft. Nature Energy 2019;4(2):160–166. https://doi.org/10.1038/s41560-018-0294-x.
- [33] Scholz, A.E., Trifonov, D., Hornung, M. Environmental life cycle assessment and operating cost analysis of a conceptual battery hybrid-electric transport aircraft. CEAS Aeronautical Journal 2022;13(1):215–235. https://doi.org/10.1007/s13272-021-00556-0.
- [34] Rajamani, R., Mracek Diedrich, A. SAE Edge Research Report: Unsettled Issues Regarding the Certification of Electric Aircraft. United States: SAE International; 2021. ISBN 978-1-4686-0323-1
- [35] Abada, S., Marlair, G., Lecocq, A., Petit, M., Sauvant-Moynot, V., Huet, F. Safety focused modeling of lithium-ion batteries: A review. Journal of Power Sources 2016;306:178–192. https://doi.org/10.1016/j.jpowsour.2015.11.100.
- [36] Bubbico, R., Greco, V., Menale, C. Hazardous scenarios identification for li-ion secondary batteries. Safety Science 2018;108:72–88. https://doi.org/10.1016/j.ssci. 2018.04.024.
- [37] Wilken, A., Pick, M., Sieb, P., Bien, M., Lobitz, L., Rodeck, R., Wicke, K., Wende, G., Friedrichs, J., Heimbs, S. Hybrid electric propulsion systems for medium-range aircraft from a maintenance point of view. 2023. https://doi.org/10.25967/610884
- [38] Bien, M., Göing, J., Friedrichs, J., Ziaja, K., Di Mare, F., Blanken, N., Cao, Y., Mertens, A., Ponick, B., Schuchard, L., Voigt, M., Mailach, R. Modelling degradation mechanisms in hybrid-electric aircraft propulsion systems. 2021.
- [39] Bien, M., Göing, J., Lück, S., Schefer, H., Friedrichs, J., Henke, M., Mallwitz, R. Parallel hybrid-electric operation of a turbofan engine during climb and the influence on stability and mro. International Journal of Gas Turbine, Propulsion and Power Systems 2024;15.
- [40] Schuchard, L., Bień, M., Ziaja, K., Blanken, N., Göing, J., Friedrichs, J., Di Mare, F., Ponick, B., Mailach, R. A study on quantities driving maintenance, repair, and overhaul for hybrid-electric aeroengines. Journal of Engineering for Gas Turbines and Power 2024;146(2). https://doi.org/10.1115/1.4063580.
- [41] Aircraft Commerce, A320 family maintenance analysis & budget. Aircraft Commerce 2006; February/March 2006(Issue No. 44):18–31. https://www.aircraftcommerce.com/display_this_article/?acm_articlekey = 26472548.
- [42] McGuire, S. The changing landscape of the aircraft industry. 2011. https://www.chathamhouse.org/sites/default/files/0711bp_mcguire.pdf.
- [43] Nowlan, F.S., Heap, H.F. Reliability-Centered Maintenance. San Francisco, California: U.S. Department; 1978. https://www.omdec.com/wikifiles/ nowlanHeap.pdf.
- [44] Deutsches Institut f
 ür Normung e.V, Din 31051:2012 grundlagen der instandhaltung. 2012. https://doi.org/10.31030/3048531.
- [45] Deutsches Institut f
 ür Normung e.V, Din en 13306:2010 instandhaltung: Begriffe der instandhaltung. 2010. https://doi.org/10.31030/2641990.
- [46] Spencer, F. Visual inspection research project report on benchmark inspections. 1996. https://doi.org/10.21949/1403546.
- [47] Sieb, P., Meissner, R., Voth, V., Kranich, F., Wicke, K., Wende, G. Design for maintenance and how it impacts life-cycle costs for aircraft systems: Comprehensive step-by-step guide for development engineers Unpublished.
- [48] Zhang, H., Hu, D., Ye, X., Chen, X., He, Y. Experimental and analytical modelling on aeroengine blade foreign object damage. International Journal of Impact Engineering 2024;183:104813. https://doi.org/10.1016/j.ijimpeng.2023.104813.
- [49] Birolini, A. Reliability Engineering: Theory and Practice. 8th edition ed.; Berlin and Heidelberg: Springer; 2017. ISBN 978-3-662-54208-8. http://www.springer.com/. https://doi.org/10.1007/978-3-662-54209-5.
- [50] Gaspari, F., Trainelli, L., Rolando, A., Perkon, I. Concept of modular architecture for hybrid electric propulsion of aircraft: Deliverable d1.1: Mahepa. 2017. https://mahepa.eu/wp-content/uploads/2017/12/D1.1-Conceptof-Modular-Architecture-fro-Hybrid-Electric-Propulsion-of-Aircraft.pdf.
- [51] Krasich, M. How to estimate and use mttf/mtbf: Would the real mtbf please stand up? in: 2009 Annual Reliability and Maintainability Symposium. IEEE. ISBN 978-1-4244-2508-2; 2009: 353–359. https://doi.org/10.1109/RAMS.2009.4914702.
- [52] Airbus, A320 family: the most successful aircraft family ever: Facts & figures. 2025 [accessed 15 August 2025]. https://www.airbus.com/sites/g/files/jlcbta136/files/2025-04/Airbus-A320-Family-Facts-and-Figures-April-2025.pdf.
- [53] Hardiman, J. The world's most flown airbus a320s. 2021 [accessed 15 August 2025]. https://simpleflying.com/the-worlds-most-flown-airbus-a320s/.
- [54] Ilarslan, M., Ungar, L.Y. Mitigating the impact of false alarms and no fault found events in military systems. in: 2015 IEEE AUTOTESTCON. IEEE. ISBN 978-1-4799-8190-8; 2015: 45-46. https://doi.org/10.1109/AUTEST.2015.7356464.
- [55] Pelham, J. What are the safety implications of no fault found? 2020 [accessed 28 March 2025]. https://insights.cranfield.ac.uk/blog/what-are-the-safety-implications-of-no-fault-found.
- [56] Airbus a320 aircraft characteristics, airport and maintenance planning. 2020. https://aircraft.airbus.com/sites/g/files/jlcbta126/files/2025-01/AC_A320_0624.pdf.
- [57] Aircraft Commerce, Cfm56-5b maintenance management & reserves. Aircraft Commerce 2014; February/March 2014 (Issue No. 92): 26–36. https://www.aircraft-commerce.com/display.this_article/?acm_articlekey=9998063.
- [58] Aircraft Commerce, Cfm56-5a/-5b maintenance analysis & budget. Aircraft Commerce 2007; February/March 2007 (Issue No. 50):15-27. https://www.aircraft-commerce.com/display_this_article/?acm_articlekey=26472697.
 [59] Meissner, R., Sieb, P., Kensbock, J.P., Wicke, K., Wende, G. Estimating the
- [59] Meissner, R., Sieb, P., Kensbock, J.P., Wicke, K., Wende, G. Estimating the scheduled maintenance implications for a hydrogen-powered aircraft. 13th EASN Conference 2023.

- [60] Aigner, B., Nollmann, M., Stumpf, E. Design of a hybrid electric propulsion system within a preliminary aircraft design software environment. 2018. https://doi.org/ 10.25967/480153.
- [61] Anker, M.A., Hartmann, C., Nøland, J.K. Feasibility of Battery-Powered Propulsion Systems for All-Electric Short-Haul Commuter Aircraft. 2023. https://doi.org/10. 36227/techrxiv.23634597.
- [62] Clarke, M.A., Alonso, J.J. Forecasting the operational lifetime of electric aircraft through battery degradation modeling. AIAA SCITECH 2022 Forum 2022; https://doi.org/10.2514/6.2022-1996.
- [63] Wu, W., Wang, S., Wu, W., Chen, K., Hong, S., Lai, Y. A critical review of battery thermal performance and liquid based battery thermal management. Energy Conversion and Management 2019;182:262–281. https://doi.org/10.1016/ i.encomman.2018.12.051.
- [64] Asli, M., König, P., Sharma, D., Pontika, E., Huete, J., Konda, K.R., Mathiazhagan, A., Xie, T., Höschler, K., Laskaridis, P. Thermal management challenges in hybrid-electric propulsion aircraft. Progress in Aerospace Sciences 2024;144:100967. https://doi.org/10.1016/j.paerosci.2023.100967.
- [65] Bertorelli, P. Pipistrel velis electro: Certified electric. 2022 [accessed 28 March 2025]. https://www.aviationconsumer.com/aircraftreviews/pipistrel-velis-electro-certified-electric/.
- [66] Gandoman, F.H., Jaguemont, J., Goutam, S., Gopalakrishnan, R., Firouz, Y., Kalogiannis, T., Omar, N., van Mierlo, J. Concept of reliability and safety assessment of lithium-ion batteries in electric vehicles: Basics, progress, and challenges. Applied Energy 2019;251:113343. https://doi.org/10.1016/j.apenergy. 2019.113343.
- [67] Briere, D., Traverse, P. Airbus a320/a330/a340 electrical flight controls a family of fault-tolerant systems. In: FTCS-23 The Twenty-Third International Symposium on Fault-Tolerant Computing. IEEE Comput. Soc. Press. ISBN 0-8186-3680-7; 1993: 616–623. https://doi.org/10.1109/FTCS.1993.627364.
- [68] Schumann, L. Reduktion des energiebedarfs mittels eines batterieelektrischen antriebs am beispiel eines kleinflugzeugs. Ph.d. thesis; University of Stuttgart; 2018. https://doi.org/10.18419/opus-9750.
- [69] Jux, B., Foitzik, S., Doppelbauer, M. A standard mission profile for hybrid-electric regional aircraft based on web flight data. 2018 IEEE International Conference on Power Electronics, Drives and Energy Systems (PEDES). IEEE. ISBN 978-1-5386-9316-2; 2018: 1–6. https://doi.org/10.1109/PEDES.2018.8707564.
- [70] Sahoo, S., Zhao, X., Kyprianidis, K. A review of concepts, benefits, and challenges for future electrical propulsion-based aircraft. Aerospace 2020;7(4):44. https://doi. org/10.3390/aerospace7040044.
- [71] Song, Z., Liu, C. Energy efficient design and implementation of electric machines in air transport propulsion system. Applied Energy 2022;322:119472. https://doi. org/10.1016/j.apenergy.2022.119472.
- [72] Massachusetts Institute of Technology. A guide to understanding battery specifications. 2008. http://web.mit.edu/evt/summary_battery_specifications.pdf.
- [73] Gandoman, F.H., Ahmed, E.M., Ali, Z.M., Berecibar, M., Zobaa, A.F., Abdel Aleem, S.H.E. Reliability evaluation of lithium-ion batteries for e-mobility applications from practical and technical perspectives: A case study. Sustainability 2021;13(21):11688. https://doi.org/10.3390/su132111688.
- [74] Karadotcheva, E., Nguyen, S.N., Greenhalgh, E.S., Shaffer, M.S.P., Kucernak, A.R.J., Linde, P. Structural power performance targets for future electric aircraft. Energies 2021;14(19):6006. https://doi.org/10.3390/en14196006.
- [75] Ebersberger, J., Fauth, L., Keuter, R., Cao, Y., Freund, Y., Hanke-Rauschenbach, R., Ponick, B., Mertens, A., Friebe, J. Power distribution and propulsion system for an all-electric short-range commuter aircraft—a case study. IEEE Access 2022;10:114514–114539. https://doi.org/10.1109/ACCESS.2022.3217650.
- [76] Stückl, S. Methods for the design and evaluation of future aircraft concepts utilizing electric propulsion systems. Ph.d. thesis; Universitätsbibliothek der TU München; München; 2016.
- [77] Staack, I., Sobron, A., Krus, P. The potential of full-electric aircraft for civil transportation: from the breguet range equation to operational aspects. CEAS Aeronautical Journal 2021;12(4):803–819. https://doi.org/10.1007/s13272-021-00530-w.
- $[78] \ \ Panasonic, Lithium ion ncr18650pf. \ 2016 \ [accessed 28 \ March 2025]. \ https://actec. \ dk/media/documents/70FC46554038.pdf.$
- [79] Panasonic, Introduction of ncr18650pf. 2013 [accessed 28 March 2025]. https://www.akkuparts24.de/mediafiles/Datenblaetter/Panasonic/Panasonic%20NCR-18650PF.pdf.
- [80] Chin, J., Schnulo, S.L., Miller, T., Prokopius, K., Gray, J.S. Battery performance modeling on sceptor x-57 subject to thermal and transient considerations. AIAA Scitech 2019 Forum 2019;https://doi.org/10.2514/6.2019-0784.
- [81] Ng, W., Datta, A. Hydrogen fuel cells and batteries for electric-vertical takeoff and landing aircraft. Journal of Aircraft 2019;56(5):1765–1782. https://doi.org/ 10.2514/1.C035218.
- [82] Jäger, F., Bertram, O., Lübbe, S.M., Bismark, A.H., Rosenberg, J., Bartscht, L. Battery-electric powertrain system design for the horizonuam multirotor air taxi concept, 2023. https://doi.org/10.48550/arXiv.2309.10631.
- [83] Vratny, P.C., Gologan, C., Pornet, C., Isikveren, A.T., Hornung, M. Battery pack modeling methods for universally-electric aircraft. CAES Air & Space Conference -FTF Congress 2013 2013;.
- [84] Jonas Ludowicy, Victor Bahrs, Martin Staggat, Feasibility studies for a medium size regional aircraft with battery powered propulsion system. 2023. https://doi.org/ 10.13009/EUCASS2023-493.
- [85] Pettes-Duler, M., Roboam, X., Sareni, B. Integrated optimal design for hybrid electric powertrain of future aircrafts. Energies 2022;15(18):6719. https://doi.org/10.3390/en15186719.

- [86] Schefer, H., Fauth, L., Kopp, T.H., Mallwitz, R., Friebe, J., Kurrat, M. Discussion on electric power supply systems for all electric aircraft. IEEE Access 2020;8:84188–84216. https://doi.org/10.1109/ACCESS.2020.2991804.
- [87] Edge, J.S., O'Kane, S., Prosser, R., Kirkaldy, N.D., Patel, A.N., Hales, A., Ghosh, A., Ai, W., Chen, J., Yang, J., Li, S., Pang, M.C., Bravo Diaz, L., Tomaszewska, A., Marzook, M.W., Radhakrishnan, K.N., Wang, H., Patel, Y., Wu, B., Offer, G.J. Lithium ion battery degradation: what you need to know. Physical chemistry chemical physics: PCCP 2021;23(14):8200–8221. https://doi.org/10.1039/D1CP00359C.
- [88] Schmalstieg, J., Käbitz, S., Ecker, M., Sauer, D.U. A holistic aging model for li(nimnco)o2 based 18650 lithium-ion batteries. Journal of Power Sources 2014;257:325–334. https://doi.org/10.1016/j.jpowsour.2014.02.012.
- [89] Clarke, M., Alonso, J.J. Lithium-ion battery modeling for aerospac e applications. Journal of Aircraft 2021;58(6):1323–1335. https://doi.org/ 10.2514/1.C036209.
- [90] Xu, B., Oudalov, A., Ulbig, A., Andersson, G., Kirschen, D.S. Modeling of lithiumion battery degradation for cell life assessment. IEEE Transactions on Smart Grid 2018;9(2):1131–1140. https://doi.org/10.1109/TSG.2016.2578950.
- [91] Sharif Azadeh, S., Vester, J., Maknoon, M.Y. Electrification of a bus system with fast charging stations: Impact of battery degradation on design decisions. Transportation Research Part C: Emerging Technologies 2022;142:103807. https: //doi.org/10.1016/j.trc.2022.103807.
- [92] Balack Philip, Atanasov Georgi, Zill Thomas. Architectural trade-offs for a hybridelectric regional aircraft. 2023. https://doi.org/10.13009/EUCASS2023-463.
- [93] Justin, C.Y., Payan, A.P., Briceno, S.I., German, B.J., Mavris, D.N. Power optimized battery swap and recharge strategies for electric aircraft operations. Transportation Research Part C: Emerging Technologies 2020;115:102605. https://doi.org/10. 1016/j.trc.2020.02.027.
- [94] Schmidt, M., Paul, A., Cole, M., Ploetner, K.O. Challenges for ground operations arising from aircraft concepts using alternative energy. Journal of Air Transport Management 2016;56:107–117. https://doi.org/10.1016/j.jairtraman. 2016.04.023.
- [95] Jain, A., Martinetti, A., van Dongen, L. Mapping the needs of design for maintenance in electric aviation. SSRN Electronic Journal 2021;https://doi.org/10.2139/ ssrn_3945107
- [96] van Oosterom, S., Mitici, M. Optimizing the battery charging and swapping infrastructure for electric short-haul aircraft—the case of electric flight in norway. Transportation Research Part C: Emerging Technologies 2023;155:104313. https://doi.org/10.1016/j.trc.2023.104313.
- [97] Jalkanen, K., Karppinen, J., Skogström, L., Laurila, T., Nisula, M., Vuorilehto, K. Cycle aging of commercial nmc/graphite pouch cells at different temperatures. Applied Energy 2015;154:160–172. https://doi.org/10.1016/j.apenergy.2015.04. 110.
- [98] Airbus a 320 atra (d-atra). 2024 [accessed 28 March 2025]. https://www.dlr.de/de/forschung-und-transfer/forschungsinfrastruktur/grossforschungsanlagen/a320-atra.
- [99] Shu, X., Yang, W., Guo, Y., Wei, K., Qin, B., Zhu, G. A reliability study of electric vehicle battery from the perspective of power supply system. Journal of Power Sources 2020;451:227805. https://doi.org/10.1016/j.jpowsour.2020.227805.
- [100] Schildt, P., Braun, C., Marzocca, P. Metric evaluating potentials of condition-monitoring approaches for hybrid electric aircraft propulsion systems. CEAS Aeronautical Journal 2020;11(1):177–190. https://doi.org/10.1007/s13272-019-00411-3.
- [101] Bennett, J.W., Mecrow, B.C., Atkinson, D.J., Atkinson, G.J. Safety-critical design of electromechanical actuation systems in commercial aircraft. IET Electric Power Applications 2011;5(1):37. https://doi.org/10.1049/iet-epa.2009.0304.
- [102] Saridakis, S., Papanikolaou, N., Voglitsis, D., Koutroulis, E., Tatakis, E., Christidis, G., Karatzaferis, I. Reliability analysis for a waste heat recovery power electronic interface applied at all-electric aircrafts. 2015 International Conference on Electrical Systems for Aircraft, Railway, Ship Propulsion and Road Vehicles (ESARS). IEEE. ISBN 978-1-4799-7400-9; 2015: 1–6. https://doi.org/10.1109/FSARS.2015.7101530
- [103] Swanke, J.A., Jahns, T.M. Reliability analysis of a fault-tolerant integrated modular motor drive for an urban air mobility aircraft using markov chains. IEEE Transactions on Transportation Electrification 2022;8(4):4523–4533. https://doi. org/10.1109/TTE.2022.3183933.
- [104] Siadatan, A., Kalantarikhalilabad, A., Rezaei-Zare, A. Reliability and fault-tolerance assessment of pmsm drive for electric aircraft applications. 2023 IEEE International Electric Machines & Drives Conference (IEMDC). IEEE. ISBN 979-8-3503-9899-1; 2023: 1–7. https://doi.org/10.1109/IEMDC55163.2023.10238884.
- [105] Kammermann, J., Bolvashenkov, I., Tran, K., Herzog, H.G., Frenkel, I. Feasibility study for a full-electric aircraft considering weight, volume, and reliability requirements. 2020 International Conference on Electrotechnical Complexes and Systems (ICOECS). IEEE. ISBN 978-1-7281-9116-4; 2020: 1–6. https://doi.org/10.1109/ ICOECS50468.2020.9278461.
- [106] Darmstadt, P.R., Catanese, R., Beiderman, A., Dones, F., Chen, E., Mistry, M.P., Babie, B., Beckman, M., Preator, R. Hazards analysis and failure modes and effects hazards analysis and failure modes and effects criticality analysis (fmeca) of four concept vehicle propulsion systems. 2019. https://ntrs.nasa.gov/citations/ 20190026443.

- [107] Cao, W., Mecrow, B.C., Atkinson, G.J., Bennett, J.W., Atkinson, D.J. Overview of electric motor technologies used for more electric aircraft (mea). IEEE Transactions on Industrial Electronics 2012;59(9):3523–3531. https://doi.org/10.1109/TIE. 2011.2165453
- [108] Quanterion Solutions Incorporated, Quanterion automated databook (nprd-2016, fmd-2016, eprd-2014). 2016 [accessed 28 March 2025]. https://www.quanterion.com/reliability-databooks/
- [109] Burgos, R., Chen, G., Wang, F., Boroyevich, D., Odendaal, W.G., van Wyk, J.D. Reliability-oriented design of three-phase power converters for aircraft applications. IEEE Transactions on Aerospace and Electronic Systems 2012;48(2):1249–1263. https://doi.org/10.1109/TAES.2012.6178060.
- [110] Aten, M., Towers, G., Whitley, C., Wheeler, P., Clare, J., Bradley, K. Reliability comparison of matrix and other converter topologies. IEEE Transactions on Aerospace and Electronic Systems 2006;42(3):867–875. https://doi.org/10.1109/TAES.2006. 248190
- [111] Bhardwaj, U., Teixeira, A.P., Soares, C.G. Reliability prediction of an offshore wind turbine gearbox. Renewable Energy 2019;141:693–706. https://doi.org/10.1016/ j.renene.2019.03.136.
- [112] Spinato, F., Tavner, P.J., van Bussel, G., Koutoulakos, E. Reliability of wind turbine subassemblies. IET Renewable Power Generation 2009;3(4):387. https://doi.org/ 10.1049/iet-rpg.2008.0060.
- [113] Tavner, P.J., Xiang, J., Spinato, F. Reliability analysis for wind turbines. Wind Energy 2007;10(1):1–18. https://doi.org/10.1002/we.204.
- [114] Smolders, K., Long, H., Feng, Y., Tavner, P.J. Reliability analysis and prediction of wind turbine gearboxes. European Wind Energy Conference EWEC 2010 2010;Volume 4. https://www.researchgate.net/publication/303578476_Reliability_Analysis_and_Prediction_of_Wind_Turbine_Gearboxes.
- [115] Atr turboprop aircraft family. 2024 [accessed 28 March 2025]. https://www.atr-aircraft.com/aircraft-services/aircraft-family/.
- [116] Aircraft Commerce, Atr 42 & 72 maintenance analysis & budget. Aircraft Commerce 2006; December 2006 / January 2007 (Issue No. 49):12–20.
- [117] Bugaj, M., Urminský, T., Rostáš, J., Pecho, P. Aircraft maintenance reserves new approach to optimization. Transportation Research Procedia 2019;43:31–40. https://doi.org/10.1016/j.trpro.2019.12.016.
- [118] Stoll, A.M., Veble Mikic, G. Design studies of thin-haul commuter aircraft with distributed electric propulsion. 16th AIAA Aviation Technology, Integration, and Operations Conference 2016;https://doi.org/10.2514/6.2016-3765.
- [119] Venditti, B. Visualized: How much do ev batteries cost? 2023 [accessed 28 March 2025]. https://www.visualcapitalist.com/visualized-how-much-do-ev-batteries-cost/.
- [120] Bubeck, S., Tomaschek, J., Fahl, U. Perspectives of electric mobility: Total cost of ownership of electric vehicles in germany. Transport Policy 2016;50:63–77. https://doi.org/10.1016/j.tranpol.2016.05.012.
- [121] Mauler, L., Duffner, F., Zeier, W.G., Leker, J. Battery cost forecasting: a review of methods and results with an outlook to 2050. Energy & Environmental Science 2021;14(9):4712–4739. https://doi.org/10.1039/D1EE01530C.
- [122] Aptsiauri, G. Concepts of full-electric and hybrid-electric propulsion and operation risk motivated integrity monitoring for future unmanned cargo aircraft. In: Dauer, J.C., ed. Automated Low-Altitude Air Delivery. Research Topics in Aerospace; Cham: Springer International Publishing. ISBN 978-3-030-83143-1; 2022: 185-204. https://doi.org/10.1007/978-3-030-83144-8_8.
- [123] Aircraft Commerce, Owner's & operator's guide: Cfm56-5a/-5b. Aircraft Commerce 2007;February/March 2007(Issue No. 50):6–29.
- [124] Wang, J. Research on civil aircraft direct maintenance cost analysis and optimization based on data mining. Journal of Physics: Conference Series 2021;1992(4):042075. https://doi.org/10.1088/1742-6596/1992/4/042075.
- [125] Aircraft Commerce, Apu maintenance & management. Aircraft Commerce 2016; December 2016 / January 2017 (Issue No. 109):55–62.
- [126] S1000d. 2024. https://s1000d.org/.
- [127] Federal Aviation Administration. Joint aircraft system/component code: Table and definitions. 2008. https://sdrs.faa.gov/documents/JASC_Code.pdf.
- [128] Bonnett, A., Yung, C. Increased efficiency versus increased reliability. IEEE Industry Applications Magazine 2008;14(1):29–36. https://doi.org/10.1109/MIA. 2007.909802.
- [129] Barzkar, A., Ghassemi, M. Electric power systems in more and all electric aircraft: A review. IEEE Access 2020;8:169314–169332. https://doi.org/10.1109/ACCESS. 2020.3024168.
- [130] Cano, T.C., Castro, I., Rodriguez, A., Lamar, D.G., Khalil, Y.F., Albiol-Tendillo, L., Kshirsagar, P. Future of electrical aircraft energy power systems: An architecture review. IEEE Transactions on Transportation Electrification 2021;7(3):1915–1929. https://doi.org/10.1109/TTE.2021.3052106.
- [131] Barzkar, A., Ghassemi, M. Components of electrical power systems in more and all-electric aircraft: A review. IEEE Transactions on Transportation Electrification 2022;8(4):4037–4053. https://doi.org/10.1109/TTE.2022.3174362.
- [132] Gerssen-Gondelach, S.J., Faaij, A.P. Performance of batteries for electric vehicles on short and longer term. Journal of Power Sources 2012;212:111–129. https:// doi.org/10.1016/j.jpowsour.2012.03.085.
- [133] Villacis, S., Rahn, A. Towards sustainable aviation: End-of-life scenarios for lithiumion batteries used in hybrid electric aircraft. Procedia CIRP 2025;135:1252–8. https://doi.org/10.1016/j.procir.2024.12.134.